Study of Glutathione-S-Transferases in Glutathione associated conjugation with Isopentenyl Pyrophosphate and Adenine Intermediates

J. Ashwin Kumar

MS14181

A dissertation submitted for the partial fulfillment of BS-MS dual degree in Science.

Indian Institute of Science Education and Research Mohali

April 2019

Certificate of Examination

This is to certify that the dissertation titled 'Study of Glutathione-S-Transferases in Glutathione associated conjugation with Isopentenyl Pyrophosphate and Adenine Intermediates' submitted by Mr. J. Ashwin Kumar (Reg. No. MS14181) for the partial fulfillment of BS-MS dual degree programme of the Institute, has been examined by the thesis committee duly appointed by the Institute. The committee finds the work done by the candidate satisfactory and recommends that the report be accepted.

Dr. Shravan Kumar Mishra Dr. Rachna Chaba Prof. Anand Kumar Bachhawat

(Supervisor)

Dated: April 26, 2019

Declaration

The work presented in this dissertation has been carried out by me under the guidance of Prof. Anand Kumar Bachhawat at the Indian Institute of Science Education and Research, Mohali.

This work has not been submitted in part or in full for a degree, a diploma, or a fellowship to any other university or institute. Whenever contributions of others are involved, every effort is made to indicate this clearly, with due acknowledgement of collaborative research and discussions. This thesis is a bonafide record of original work done by me and all sources listed within have been detailed in the bibliography.

J. Ashwin Kumar

April 26, 2019

In my capacity as the supervisor of the candidate's project work, I certify that the above statements by the candidate are true to the best of my knowledge.

Prof. Anand Kumar Bachhawat

(Thesis supervisor)

Acknowledgement

“Life is like riding. To keep your balance, you must keep moving”

- Albert Einstein

Bicycling is one activity that I always fancied during my childhood. Before I actually learned to ride a bicycle, it seemed the most difficult thing to balance oneself on two thin wheels. I always wondered how easily people were not only riding but doing a variety of stunt like paddling and sitting on cycle seat with a jump, riding without holding handle etc. In my initial days of bicycle training, my father used to hold bicycle from behind while I used to paddle. I got similar support from Prof. Anand K. Bachhawat and Prof. Samir K. Brahmachari who didn’t let me fall/surrender when I was in initial state of my research career, I am fortunate to have them both during my BS-MS. journey.

I would like to express my deep gratitude to Prof. Anand K. Bachhawat, my supervisor for his patient guidance, enthusiastic encouragement, and valuable suggestions. He was always available for discussions, helping and supporting me at all times. He has given me immense freedom in my work and has always encouraged me to think independently and to design experiments on my own. This project would have never been so fruitful without the help and support of my lab members. I would like to mention my special thanks to senior members of the lab for their guidance and continuous support. Whenever I needed help with any experiment or got stuck they were always there to help me. They were also available for discussing work all the time and it always helped me to get new insights into my work.

Next, I would like to thank, the younger lab members for their enthusiastic participation for discussion about the work. They always shared their experience with any experiments and gave the best ideas when something went wrong. Mr. Nithishwer M. A., Mr. Rakesh Pandian, Mr. Devang Haresh Liya, Dr. Mukta Sharma, Mr. Nitish Tayal and Mr. Shubham Kumar Sinha have been there to help me whenever needed. I would like to thank all of them for making this research experience a memorable one. I would like to thank my friends Mr. Ravineet Yadav and Ms. Anupreet Saini for their continuous support in good and bad times. A sincere thanks to all DBS faculty members and iGEM IISER-Mohali community, all colleagues and teaching stuffs for their help.

Finally I would like to thank a very special person, Mr. Mayank Kamboj, whose principles influenced me a lot and helped me shape myself. This dissertation is dedicated to him.

J. Ashwin Kumar

List of figures

List of tables

Abbreviations

GSH	Glutathione
GST	Glutathione-S-Transferase
AIR	Phosphoribosylaminoimidazole
CAIR	Phosphoribosylaminoimidazole carboxylate
3-MBG	3-methylbutanol-glutathione
3-MBCG	3-methylbutanol-cysteinylglycine
DMSO	Dimethyl sulfoxide

Contents

Chapter 2: Materials and methods [11]

SECTION A: Materials

2.1 Chemicals and Reagents

2.2 Strains and Plasmids

2.3 Oligonucleotides

2.4 Media

2.4.1 LB Medium

2.4.2 YPD Medium

2.4.3 SD Medium

2.5 BUFFERS AND STOCK SOLUTIONS

2.5.1 Ampicillin (100 mg/mL) and Chloramphenicol (25 mg/mL) stock solutions.

2.5.2 Glutathione Stock Solution (100mM)

2.5.3 50% Glycerol (used for preparing –80°C stocks of *E. coli*)

2.5.3 25% Glycerol (used for preparing –80°C stocks of *S. cerevisiae*)

2.5.4 IPTG (Isopropyl β-D-1-thiogalactopyranoside) stock solution (500mM)

2.5.5 Alkaline Lysis Buffers (Plasmid DNA preparation from *E. coli*)

2.5.6 Agarose Gel Electrophoresis Reagents

2.5.7 Solutions for preparation of chemical competent *E. Coli* cells

2.5.8 Yeast Transformation Solutions (*S. cerevisiae*)

2.5.9 Breaking buffer for genomic DNA isolation from yeast

2.5.10 SDS-PAGE Solutions and Reagents

2.5.11 Immunoblotting (Western Blotting) Reagents

SECTION B: METHODS

2.6 Growth and maintenance of bacteria and yeast strains

2.7 Recombinant DNA methodology (restriction digestion, ligation, transformation of *E. coli*. PCR amplification, etc)

2.8 Transformation of yeast

2.9 Construction of *ade1/ade2:* URA/HIS disruption cassette

2.10 Construction of yeast strains used in the study: disruption of ADE1/ADE2 gene in different *S. cerevisiae* gene deletion strains

2.11 Isolation of genomic DNA from yeast

2.12 Growth assay by dilution spotting

2.13 Recombinant expression and purification of His-tagged GSTM3 and Grx4 protein in *E. coli*

2.14 Protein concentration and quantification

2.15 Gel filtration analysis of proteins

2.16 Western blot analysis of C-terminal HA tagged GSTM3

2.17 Extraction of Felinine and Sample preparation for HPLC

2.18 Mass spectrometry analysis of the purified Felinine

2.19 Enzyme Assay and Kinetics

2.20 Sequence analysis

Chapter 3: The ade pigmentation of yeast: Uncovering missing links in the pathway [35]

3.1.1 Introduction

3.1.2 A detailed description of the ADE pathway in S. cerevisiae

3.1.3 ‘AIR’ and ‘CAIR’ Intermediates in adenine biosynthesis

3.1.4 Transporters involved in the AIR/CAIR detoxification pathway

3.1.5 Adenine biosynthesis pathway activation in ade1 / ade2 mutants:

3.2 Objective

3.3 Results and Discussion

3.3.1 Identification of Putative GST involved in GS-AIR/CAIR conjugation:

3.3.2 Evaluation of the role of the different thioredoxin superfamily members in the ade pigment formation

3.3.3 Effect of GSH on the red pigmentation

3.3.4 Effect of different adenine concentration on growth and red pigmentation

3.3.5 Effect of temperature on the red pigmentation

3.3.6 Complementation by GRX4 restores the pigmentation of grx4Δ in ade2Δ background

3.3.7 A Color table illustrating the pigmentation at different ADE concentrations

3.3.8 Investigating the role of post-vacuolar processing of AIR / CAIR-GSH in pigment formation

3.3.9 Investigating the involvement of the vacuolar peptidases involved in red pigmentation in vacuole

3.3.10 Involvement of ECM38 in post-vacuolar processing of the CAIR / AIR – GSH conjugate

3.3.11 Predicted players involved in the red pigmentation in vacuole (ade Δ)

3.4 Conclusion

Chapter 4: Reconstructing biosynthetic pathway of the cat pheromone, felinine in yeast [51]

4.1 Introduction

4.1.1 Felinine – Properties and uses

4.1.2 Locations of the putative enzymes involved in felinine biosynthesis in the cat renal system

4.1.3 Felinine biosynthesis in cats

4.1.4 Predicting a probable felinine biosynthesis pathway in S. cerevisiae

4.1.5 Localizations of yeast enzymes which play a role in felinine synthesis

4.2 Objective

4.3 Results and Discussions

4.3.1 Identification of putative Glutathione-S-Transferase (GST) involved in felinine pathway that conjugates IPP with GSH

4.3.2 GSTM3 picked as a putative GST involved in felinine biosynthesis based on tissue metabolites localizations

4.3.3 Experimental approach for reconstructing the felinine pathway in yeast

4.3.3.1 Codon optimization, custom synthesis and cloning of GSTM3 gene from Felis catus into the yeast expression vector

4.3.3.2 Validation for GSTM3 expression in Saccharomyces cerevisiae

4.3.3.3 Protein purification and In vitro analysis of the GST conjugation

4.3.3.4 Protein purification and In vitro analysis of the GST conjugation.

4.3.3.5 In vitro enzymatic assay to check GSTM3 activity with GSH and IPP

Abstract

Glutathione-S-transferases (GSTs) are a superfamily of homo- and hetero-dimeric proteins that mediate the catalytic binding of glutathione to an array of endo- and exobiotic compounds as a general detoxification scheme. In this study we have investigated the role of GSTs in two different projects.

(i) In the first project we looked into the putative Glutathione-S-Transferases (GSTs) involved in the conjugation of Isopentenyl pyrophosphate (IPP) to glutathione. In this work we attempted to reconstruct the *Felis catus'* Felinine biosynthetic pathway in *Saccharomyces cerevisiae*. Glutathione (GSH) and IPP conjugates to give 3-MBG in cat (*Felis catus*), the precursor to felinine. The enzyme catalyzing the felinine is exclusive to cats. Through bioinformatics analysis and literature mining, we have shortlisted a putative cat GST candidate GSTM3. The putative GST candidate GSTM3 was cloned and expressed in yeast was shown to conjugate with and IPP through *in-vitro* studies and the production of felinine by the recombinant yeast was successfully validated using HPLC and HR-MS.

(ii) In the second project study the glutathione-mediated pathway for the detoxification of endogenously derived toxic compounds was investigated. The ade1 / ade2 mutants of *Saccharomyces cerevisiae*, when grown on adenine-limiting medium, accumulate a characteristic red pigment (ade pigment) in their vacuoles. The precursors of the ade pigments are toxic intermediates that form conjugates with glutathione, followed by their transport inside the vacuole. In this study, putative Glutathione-S-Transferases (GSTs) involved in this conjugation were investigated. We show that the glutaredoxin, GRX4 is the GST responsible for the AIR/CAIR conjugation to GSH. The AIR/CAIR – GSH conjugate is known to be transported into the vacuole through the various GSH conjugate pumps. We also show that, ECM38, a ϒ-glutamyl transpeptidase that can degrades GSH conjugate, by removal of glutamate is also critical for the red pigmentation.

Chapter 1: Introduction

1.1 Glutathione

Glutathione or *γ-L-glutamyl-L-cysteinyl-glycine*, is one of the most abundant thiol (-SH group) containing organic compounds in many organisms including *Saccharomyces cerevisiae* (1). Synthesized by a cytosolic process in animals and yeast, Glutathione (GSH) plays many important functions including its role in redox. In addition to these, GSH also plays a pivotal role in (i) response to sulfur and nitrogen starvation; (ii) detoxification of endogenous toxic metabolites; (iii) protection against oxidative stress provoked by exposure to reactive oxygen species; (iv) detoxification of Xenobiotics and (v) resistance to heavy-metal stress. Apart from these, it is also involved in biosynthesis of iron–sulfur proteins in the mitochondria, redox signaling, apoptosis, sulfur storage and transport (1).

1.1.1 Glutathione conjugation and conjugates

Glutathione (γ-glutamyl-L-cysteinylglycine; GSH) is present in high concentrations in most living cells and participates in a variety of vital cellular reactions (2). In particular, GSH is involved in protecting cells from potentially toxic electrophiles formed via the metabolism of xenobiotics. These reactions have long been associated with the process of detoxicating cells. Compounds that form GSH conjugates during detoxification are processed by γ-glutamyl transpeptidase (γ-GT) and dipeptidases to cysteine *S*-conjugates. In recent years, a lot of evidence indicating that GSH conjugation plays an important role in the formation of toxic metabolites from a variety of chemicals has accumulated. Thus, we know that several classes of compounds are converted, via conjugation with GSH, into either cytotoxic, genotoxic, or mutagenic metabolites. The small peptide and major cellular thiol, γ-Glutamyl-Cys-Gly (GSH), plays a crucial role in the metabolism of electrophilic chemicals through GSH conjugation reaction. The conjugation revolves around a nucleophilic displacement reaction with the GSH anion (GS–) serving as the nucleophile. For this reaction to proceed, the sulfhydryl group (–SH) on the cysteine residue of the GSH is required. These reactions are catalyzed by glutathione transferases or GSTs (3).

There are a lot of features of GSH conjugation that make them very important. For example most substrates that possess an electrophilic center such as sulfur, nitrogen or carbon, can directly conjugate with GSH whereas sugar conjugation reactions require hydrolysis or oxidation before the conjugation

reaction (3). Also another useful feature of GSH conjugation is that once a water-soluble GSH-conjugate is formed, it can easily be removed.

GSH conjugation reactions are very crucial and are involved in the bioactivation of a range of xenobiotics. The GSH-dependent bioactivation reactions can be classified into one of four types: (Type I) directly toxic GSH conjugates may be formed from vicinal dihaloalkanes via formation of electrophilic sulfur mustards: (Type II) cysteine conjugate β-lyase-dependent bioactivation is involved in the selective nephrotoxicity of haloalkenes; (Type III) GSH conjugates of hydroquinones and isothiocyanates may serve as transport and targeting metabolites; and (Type IV) GSH-dependent reactions may be involved in the release of toxic agents from precursor organic thiocyanates and nitrosoguanidines (*N*-methyl-*N′*-nitro-*N*-nitrosguanidine) (3).

1.1.2 Factors Affecting GSH Conjugation

There are a range of factors that affect the rate of GSH conjugation, among them the most influential ones are:

(i) Nucleophilic character of GSH: GSH exists as two nucleophilic species at physiological pH, its native state and as thiolate anion. Concentrations of the latter, the stronger nucleophile, are approximately 1% of GSH concentration [pKa of GSH = 9.2] (4).

(ii) Nature of Electrophilic Center: Reactions with which we are mostly concerned are nucleophilic substitutions (including opening of the strained oxirane ring) and nucleophilic additions to a polarized double bond. The mechanism of GSH conjugation may be examined in relation to the two following extremes. (a) The electrophilic center is soft (soft electrophiles), and the nucleophile initiates reaction by causing polarization of the electrophile: in these circumstances strong nucleophiles such as GSH and GS will react best. (b) The electrophilic center is hard (hard electrophiles) and capable of initiating a reaction by polarizing a weak nucleophile and therefore the reaction is less dependent on GSH (4).

1.1.3 Glutathione Conjugate Transporters

Glutathione transporters play a very important role in the detoxication pathway in cells. These pumps facilitate the Glutathione conjugates into the vacuole to dump in the toxic conjugate, while the amino acids of glutathione gets recycled into the cytoplasm. Two vacuolar localized multidrug resistance

associated proteins (MRPs) in yeasts have been shown to be able to function in low affinity glutathione transport. These are the yeast cadmium factor-1 (Ycf1p) and the bile pigment transporter-1 (Bpt1p) (5). These proteins, though primarily recognized as glutathione-conjugate ABC-dependent efflux pumps, have been shown to mediate glutathione transport into the vacuole, albeit with very low affinity (Km in millimolar range), in contrast to the affinity for glutathione disulphide and glutathione conjugates (Km in micro molar range). Between the two transporters- Ycf1p and Bpt1p, Ycf1p has greater glutathione transport capability, though Ycf1p has significantly lower affinity for glutathione (Km=15 mM), as compared to Bpt1p (Km= 3 mM) (6). Although Ycf1p and Bpt1p are known to transport Glutathione, the possibility of other transporters contributing towards GSH-conjugate or GSH transport in the vacuole is also not ruled out.

1.1.4 Glutathione degradation

Glutathione degradation is a crucial process as it facilitates its resynthesis in the cytoplasm. Degradation of glutathione is facilitated by the membrane associated enzymes γ-glutamyl transpeptidase (γ-GT/ECM38) and is followed by uptake of the constituent products (either cys–gly and glutamate or cys, gly and glutamate) and resynthesis of GSH (7). Cys–gly can be either degraded on the cell surface or vacuolar lumen or vacuolar surface by membrane bound dipeptidases or by intracellular/intravacuolar cys–gly peptidases (8) (following peptide uptake).

1.1.5 Role of Glutathione in detoxification

GSH plays a key role in cellular defense against reactive electrophiles such as halogenated aromatics. Many xenobiotics can react either spontaneously with the thiol moiety of GSH to form GSH *S*-conjugates, or via GSH *S*-transferases (GST: GSH+RX→GS-X+RH). Ycf1p appears as the major GS-X vacuolar transporter in *Saccharomyces cerevisiae* that transports the toxic glutathione conjugate into the vacuole (9).

In GSH, it is the cysteinyl residue which provides a nucleophilic thiol important for the detoxication of electrophilic metabolites and metabolically produced oxidizing agents. It's net negative charge and overall hydrophilicity greatly increases the aqueous solubility of the lipophilic moieties with which it becomes conjugated (10). The Cysteinyl residue's unique tripeptide structure, including the N-terminal glutamyl residue linked via a y-glutamyl peptide bond, provides for specificity in GSH-enzyme interaction.

1.2 Glutathione-S-Transferases (GSTs)

Glutathione-S-transferases (GSTs) are a superfamily of homo- and hetero-dimeric proteins that mediate the catalytic binding of glutathione to an array of endo- and exobiotic compounds as a general detoxification scheme (11). GSTs are involved in a broad range of cellular reactions and processes such as isomerization, reduction, transport, storage, prostaglandin biosynthesis, thiol transfer, stress kinase regulation, cell apoptosis, and peroxidase activity. Further, GSTs are responsible for the conjugation of the tripeptide glutathione (GSH) to a wide range of electrophilic substrates such as industrial pollutants, drugs, genotoxic carcinogen metabolites, antibiotics, insecticides and herbicides (12). Glutathione S-transferases (GSTs) belongs to phage II detoxification enzymes which play an important role in detoxification/biotransformation of endogenous and exogenous toxic agents like reactive oxygen species (ROS), reactive nitrogen species (RNS) and xenobiotic including environmental carcinogens (13). GSTs are currently of great interest in drug discovery, nanotechnology and green biotechnology owing to their involvement in major cellular processes.

GSTs are widely distributed in eukaryotes and prokaryotes and there have been reports indicating that they may have evolved in aerobic bacteria to protect cells against oxygen toxicity.

1.2.1 Cytosolic GSTs

GSTs can be classified into cytosolic, mitochondrial and membrane associated GSTs, with cytosolic GSTs being predominantly involved in detoxification. Cytosolic GSTs are abundantly found in all aerobic organisms and they have been studied extensively. In recent years, numerous cytosolic GST genes from mammals, insects, plants and bacteria, fungi, yeast, and fish have been identified, purified and characterized. Presently, seven classes of cytosolic GSTs are recognized in mammals (alpha, mu, omega, pi, sigma, theta, and zeta), six classes in insects (delta, epsilon, omega, sigma, theta, and zeta), six classes in plants (DHAR (dehydroascorbate), lambda, phi, tau, theta, and zeta), three classes in fungi (alpha, gamma, and mu), and five classes in bacteria (beta, chi, rho, theta, and zeta) (9). As far as genetic similarity is concerned, Cytosolic GSTs share >40% sequence identity within classes but <25% between classes (8).

1.2.2 Role of GSTs in detoxification

The biotransformation of foreign substances (xenobiotic) including drugs is divided into three different phases, namely I, II and III. The cytochrome P450 (CYPs) enzymes are major players at this phase of xenobiotics biotransformation.

The compounds that have undergone Phase I are more polar than their parent compound, thus they can go to Phase II – conjugation. Phase II enzymes are responsible for forming a highly hydrophilic compound that is readily eliminated from the cell. Reactions at this phase are performed mainly by transferases including methyltransferases, sulfotransferases, glutathione transferases, and UDP glucuronosyltransferases. The main task of these enzymes is to perform conjugation reactions such as methylation, sulfation, amino acid and glutathione conjugation, etc. The final phase of enzymatic detoxification is export – Phase III. This phase uses specific transporters to excrete the newly formed Phase II products out of the cell.

Phase II enzymes play a key role in the biotransformation of endogenous compounds and xenobiotics to easily excretable forms and also help in the metabolic inactivation of pharmacologically active substances (12). The phase II enzymes can perform biotransformation through conjugation reactions. Glutathione S-transferases (GSTs) are one of the most versatile phase II detoxification enzymes. As mentioned before, GSTs are involved in the xenobiotic metabolism and play major role in cellular protection against oxidative stress.

1.2.3 Activation of xenobiotics

As mentioned earlier, the conjugation reaction catalyzed by GST forms less reactive products that is readily excreted. In some cases, the glutathione (GSH) conjugate is more reactive than the parent compound like in the case of short chain alkyl halides that contain two functional groups and 1, 2-dihaloethanes. In such cases, the GSH conjugate rearranges to form an episulfonium intermediate which responsible for DNA modification. Similarly, The conjugation of GSH with the solvent dichloromethane facilitates formation of the highly unstable Schloromethlglutathione, which is capable of DNA modification (3).

Moderately toxic compounds like allyl-, benzyl-, phenethyl-isothiocyanates and sulforaphane are reversibly conjugated with GSH by GST to form thiocarbamates which spontaneously degrade to their isothiocyanates by releasing GSH. These isothiocyanates can then be taken up by the cell and reconjugated with GSH and then form thiocarbamate which reverts to the isothiocyanate. Due to this cyclic process, intracellular GSH levels are decreased and facilitate the distribution of isothiocyanates throughout the entire body. Such isothiocyanates either lower GSH content or stay unconjugated with GSH. When they stay unconjugated, they are more likely to revert to thiocarbalate proteins, which result in cell death (14).

1.3. Detoxification

Detoxification is a crucial metabolic process that provides protection to all living organisms against harmful agents. Glutathione transferases (GSTs; E.C. 2.5.1.18) are one of the most important families of enzymes in nature playing a significant role in cellular detoxification processes.

The classic role of GSTs is to catalyze the conjugation of non-polar compounds that contain an electrophilic center to reduced glutathione (GSH); consequently, the resultant compounds are rendered to be more soluble and easy for cellular excretion. GSTs contribute to the metabolism of pesticides, herbicide, pharmaceuticals, and other foreign compounds (xenobiotics), including products of oxidative stress, such as peroxides (15).

1.3.1 Detoxification of exogenous hazardous agents

Glutathione S-transferases (GSTs) are capable of detoxifying a large number of exogenous toxic agents like carcinogens, drugs and environmental pollutants. The chemotherapeutic agents of cancer such as adriamycin, 1, 3-bis (2-chloroethyl)-1-nitrosourea (BCNU), busulfan, carmustine, chlorambucil, cis-platin, crotonyloxymethyl-2-cyclohexenone (COMC-6), melphalan, mitozantrone, thiotepa, cyclophosphamide and ethacrynic acid are detoxified by GSTs. Environmental chemicals and their metabolites like acrolein, atrazine, DDT, inorganic arsenic, lindane, Malathion, methyl parathion, muconaldehyde and tridiphane are also detoxified by GST isoenzymes. In addition to these, GSTs also detoxify a large number of epoxides like fosfomycin and polycyclic aromatic hydrocarbons (PAHs). Activated metabolites N-aacetoxyPhIP of heterocyclic amine, 2-amino-1-methyl-6-phennylimidazo [4, 5-b] pyridine (PhIP) which produced by cooking protein-rich food is also detoxified by cytosolic GST (3).

1.3.2 Detoxification of endogenous hazardous agents

In addition to exogenous toxic agents, endogenous toxic agents also exhibit numerous deleterious effects on biological system. Theses toxic agents have a highly negative impact on molecular systems. However, the biological system has developed an efficient antioxidant enzymatic system to neutralize these threats. GSTs are multifunctional antioxidant enzymes which have non selenium glutathione (GSH) peroxidase (GPx) activity in addition to GSH transferase activity. By these two activities, GSTs detoxify a wide range of hazardous substances.

The GSTs also exhibit an important moderate role in lipid peroxidation process in biological membranes known as non-selenium glutathione peroxidase (GPx) activity. The non-selenium (GPx) shows activity with 1-palmitoyl-2-(13-hydroperoxy-cic-9, trans-11-octadecadienoyl)-L-3-phosphadylcholine, phospatidylcholinehydroperoxide and reducing lipid hydroperoxides which are in membranes. The transferases can reduce cholesterylhydroperoxides, fatty acid hydroperoxides, (S)-9-hydroproxy-10, 12-octodecadieonic acid and (S)-13-hydroperoxy-9, 11-octadecadieonic acid. Also, lipid peroxidation end products like 2-alkenals acrolein, crotonaldedyde and 4-hydroxy-2-alkenals are conjugate with GSH by GSTs. GSTs catalyze the GSH conjugation with cholesterol-5, 6-oxide, epoxyeicosatrienoic acid and 9, 10-epoxystearic acid (11). These indicate GST's role in cellular protection against oxidative stress by harmful electrophiles.

This thesis has two distinct parts, both of which relate to glutathione-S-transferases. Each of the following chapters will have its own specific introduction, followed by the objective for that chapter, results and discussion.

Chapter 2: Materials and methods

SECTION A: Materials

2.1 Chemicals and Reagents

All chemicals used were obtained from commercial sources and were of analytical grade. Media components, fine chemicals and reagents were purchased from Sigma Aldrich (St. Louis, USA), HiMedia (Mumbai, India), Merck. India Ltd (Mumbai, India), USB Corporation (Ohio, USA) or Difco, USA. Oligonucleotides (primers) were designed using SnapGene (version 2.4.3) software and were purchased from Integrated DNA Technologies (IDT). Enzymes (Restriction enzymes, T4 DNA ligase, Calf Intestinal Phosphatase (CIP), Antarctic phosphatase, *Vent* DNA polymerase, *Phusion* High-fidelity DNA polymerase and other modifying enzymes), their buffers, dNTPs, DNA and protein molecular weight markers were purchased from New England Biolabs Inc, (Beverly, MA, USA) or Thermo Scientific. Gel-extraction kits and plasmid miniprep columns were obtained from BioNEER and Promega. GSH was obtained from Sigma-Aldrich, USA.Nitrocellulose Hybond N^+ membrane (Hybond ECL) and ECL Plus Western Blotting Detection Reagents were purchased from Amersham Biosciences GE healthcare (U.K.). anti-HA mouse Tag polyclonal antibody and anti-mouse HRP-linked antibody were bought from Cell Signaling (Danvers, MA, USA).

2.2 Strains and Plasmids

Escherichia coli DH5α was used as the cloning host. BL21 (DE3) was used as expression host. The genotype for the *E. coli* and *Saccharomyces cerevisiae* strains used in the study are given in Table 2.1. The list of various plasmids used in this study is given in Table 2.2.

Table 2.1: List of bacterial and yeast strains used in the study

Strain	Genotype	Source
Escherichia coli strains		
ABE 460 (DH5α)	F $^-$ *gyr A96(Nal) recA1 relA1 endA1 thi-1 hsdR17*(r_k^- m_k^+) *gln V44 deoR Δ(lacZYA-argF) U169 [ϕ80dΔ(lacZ) M15]*	Lab strain
ABE 849 (BL21(DE3))	*F $^-$ ompThsd*SB(r_B^- m_B^-) gal dcm (DE3)	Lab strain
Saccharomyces cerevisiae strains		
ABC 733 (BY4741)	*MATa his3Δ1 leu2Δ0 met15Δ0 ura3Δ0*	Lab stock
ABC 3093	BY4741; *MATa his3Δ1 leu2Δ0 met15Δ0 ura3Δ0 grx1::kanMX4*	Lab stock
ABC 3092	BY4741; *MATa his3Δ1 leu2Δ0 met15Δ0 ura3Δ0 grx2::kanMX4*	Lab stock
ABC 3094	BY4741; *MATa his3Δ1 leu2Δ0 met15Δ0 ura3Δ0 grx3::kanMX4*	Lab stock
ABC 3095	BY4741; *MATa his3Δ1 leu2Δ0 met15Δ0 ura3Δ0 grx4::kanMX4*	Lab stock
ABC 3096	BY4741; *MATa his3Δ1 leu2Δ0 met15Δ0 ura3Δ0 grx5::kanMX4*	Lab stock
ABC 5943	BY4741; *MATa his3Δ1 leu2Δ0 met15Δ0 ura3Δ0 grx6::kanMX4*	Euroscarf
ABC 5944	BY4741; *MATa his3Δ1 leu2Δ0 met15Δ0 ura3Δ0 grx7::kanMX4*	Euroscarf

ABC 5945	BY4741; *MATa his3Δ1 leu2Δ0 met15Δ0 ura3Δ0 trx1::kanMX4*	Euroscarf
ABC 3091	BY4741; *MATa his3Δ1 leu2Δ0 met15Δ0 ura3Δ0 trx2::kanMX4*	Lab stock
ABC 5412	BY4741; *MATa his3Δ1 leu2Δ0 met15Δ0 ura3Δ0 trx3::*kanMX4	Lab stock
ABC 5946	BY4741; *MATa his3Δ1 leu2Δ0 met15Δ0 ura3Δ0 prx1::kanMX4*	Euroscarf
ABC 5947	BY4741; *MATa his3Δ1 leu2Δ0 met15Δ0 ura3Δ0 srx1::kanMX4*	Euroscarf
ABC 5948	BY4741; *MATa his3Δ1 leu2Δ0 met15Δ0 ura3Δ0 gto1::kanMX4*	Euroscarf
ABC 5949	BY4741; *MATa his3Δ1 leu2Δ0 met15Δ0 ura3Δ0 gto2::kanMX4*	Euroscarf
ABC 5950	BY4741; *MATa his3Δ1 leu2Δ0 met15Δ0 ura3Δ0 gto3::kanMX4*	Euroscarf
ABC 5951	BY4741; *MATa his3Δ1 leu2Δ0 met15Δ0 ura3Δ0 gtt1::kanMX4*	Euroscarf
ABC 5952	BY4741; *MATa his3Δ1 leu2Δ0 met15Δ0 ura3Δ0 gtt2::kanMX4*	Euroscarf
ABC 5953	BY4741; *MATa his3Δ1 leu2Δ0 met15Δ0 ura3Δ0 lap1::kanMX4*	Euroscarf
ABC 5954	BY4741; *MATa his3Δ1 leu2Δ0 met15Δ0 ura3Δ0 lap2::kanMX4*	Euroscarf
ABC 5955	BY4741; *MATa his3Δ1 leu2Δ0 met15Δ0 ura3Δ0 lap3::kanMX4*	Euroscarf

ABC 5956	BY4741; *MATa his3Δ1 leu2Δ0 met15Δ0 ura3Δ0 lap4::kanMX4*	Euroscarf
ABC 1318	BY4741; *MATa his3Δ1 leu2Δ0 met15Δ0 ura3Δ0 aap1::kanMX4*	Lab stock
ABC 1066	BY4741; *MATa his3Δ1 leu2Δ0 met15Δ0 ura3Δ0 ecm38::kanMX4*	Lab stock
ABC 1305	BY4741; *MATa his3Δ1 leu2Δ0 met15Δ0 ura3Δ0 kex1::kanMX4*	Lab stock
ABC 5957	BY4741; *MATa his3Δ1 leu2Δ0 met15Δ0 ura3Δ0 pep4::kanMX4*	Euroscarf
ABC 1281	BY4741; *MATa his3Δ1 leu2Δ0 met15Δ0 ura3Δ0 cps1::kanMX4*	Lab stock
ABC 470	BY4741; *MATa his3Δ1 leu2Δ0 met15Δ0 ura3Δ0 ycf1::kanMX4*	Lab stock
ABC 1720	BY4741; *MATa his3Δ1 leu2Δ0 met15Δ0 ura3Δ0 prc1::kanMX4*	Lab stock
ABC 1309	BY4741; *MATa his3Δ1 leu2Δ0 met15Δ0 ura3Δ0 ynl045::kanMX4*	Lab stock
ABC 1719	BY4741; *MATa his3Δ1 leu2Δ0 met15Δ0 ura3Δ0 ybr139::kanMX4*	Lab stock
ABC 5885	BY4741; *MATa his3Δ1 leu2Δ0 met15Δ0 ura3Δ0 grx1::kanMX4 ade2::HIS3*	This study
ABC 5886	BY4741; *MATa his3Δ1 leu2Δ0 met15Δ0 ura3Δ0 grx2::kanMX4 ade2::HIS3*	This study
ABC 5887	BY4741; *MATa his3Δ1 leu2Δ0 met15Δ0 ura3Δ0 grx3::kanMX4 ade2::HIS3*	This study

ABC 5888	BY4741; *MATa his3Δ1 leu2Δ0 met15Δ0 ura3Δ0 grx4::kanMX4 ade2::HIS3*	This study
ABC 5889	BY4741; *MATa his3Δ1 leu2Δ0 met15Δ0 ura3Δ0 grx5::kanMX4 ade2::HIS3*	This study
ABC 5890	BY4741; *MATa his3Δ1 leu2Δ0 met15Δ0 ura3Δ0 grx6::kanMX4 ade2::HIS3*	This study
ABC 5891	BY4741; *MATa his3Δ1 leu2Δ0 met15Δ0 ura3Δ0 grx7::kanMX4 ade2::HIS3*	This study
ABC 5892	BY4741; *MATa his3Δ1 leu2Δ0 met15Δ0 ura3Δ0 trx1::kanMX4 ade2::HIS3*	This study
ABC 5893	BY4741; *MATa his3Δ1 leu2Δ0 met15Δ0 ura3Δ0 trx2::kanMX4 ade2::HIS3*	This study
ABC 5894	BY4741; *MATa his3Δ1 leu2Δ0 met15Δ0 ura3Δ0 trx3::*kanMX4 *ade2::HIS3*	This study
ABC 5895	BY4741; *MATa his3Δ1 leu2Δ0 met15Δ0 ura3Δ0 prx1::kanMX4 ade2::HIS3*	This study
ABC 5896	BY4741; *MATa his3Δ1 leu2Δ0 met15Δ0 ura3Δ0 srx1::kanMX4 ade2::HIS3*	This study
ABC 5897	BY4741; *MATa his3Δ1 leu2Δ0 met15Δ0 ura3Δ0 gto1::kanMX4 ade2::HIS3*	This study
ABC 5898	BY4741; *MATa his3Δ1 leu2Δ0 met15Δ0 ura3Δ0 gto2::kanMX4 ade2::HIS3*	This study
ABC 5899	BY4741; *MATa his3Δ1 leu2Δ0 met15Δ0 ura3Δ0 gto3::kanMX4 ade2::HIS3*	This study
ABC 5900	BY4741; *MATa his3Δ1 leu2Δ0 met15Δ0 ura3Δ0 gtt1::kanMX4 ade2::HIS3*	This study

ABC 5901	BY4741; *MATa his3Δ1 leu2Δ0 met15Δ0 ura3Δ0 gtt2::kanMX4 ade2::HIS3*	This study
ABC 5902	BY4741; *MATa his3Δ1 leu2Δ0 met15Δ0 ura3Δ0 lap1::kanMX4 ade2::HIS3*	This study
ABC 5903	BY4741; *MATa his3Δ1 leu2Δ0 met15Δ0 ura3Δ0 lap2::kanMX4 ade2::HIS3*	This study
ABC 5904	BY4741; *MATa his3Δ1 leu2Δ0 met15Δ0 ura3Δ0 lap3::kanMX4 ade2::HIS3*	This study
ABC 5905	BY4741; *MATa his3Δ1 leu2Δ0 met15Δ0 ura3Δ0 lap4::kanMX4 ade2::HIS3*	This study
ABC 5906	BY4741; *MATa his3Δ1 leu2Δ0 met15Δ0 ura3Δ0 aap1::kanMX4 ade2::HIS3*	This study
ABC 5907	BY4741; *MATa his3Δ1 leu2Δ0 met15Δ0 ura3Δ0 ecm38::kanMX4 ade2::HIS3*	This study
ABC 5908	BY4741; *MATa his3Δ1 leu2Δ0 met15Δ0 ura3Δ0 kex1::kanMX4 ade2::HIS3*	This study
ABC 5909	BY4741; *MATa his3Δ1 leu2Δ0 met15Δ0 ura3Δ0 pep4::kanMX4 ade2::HIS3*	This study
ABC 5910	BY4741; *MATa his3Δ1 leu2Δ0 met15Δ0 ura3Δ0 cps1::kanMX4 ade2::HIS3*	This study
ABC 5911	BY4741; *MATa his3Δ1 leu2Δ0 met15Δ0 ura3Δ0 prc1::kanMX4 ade2::HIS3*	This study
ABC 5912	BY4741; *MATa his3Δ1 leu2Δ0 met15Δ0 ura3Δ0 ynl045::kanMX4 ade2::HIS3*	This study
ABC 5913	BY4741; *MATa his3Δ1 leu2Δ0 met15Δ0 ura3Δ0 ybr139::kanMX4 ade2::HIS3*	This study

ABC 5914	BY4741; *MATa his3Δ1 leu2Δ0 met15Δ0 ura3Δ0 grx1::kanMX4 ade1::URA3*	This study
ABC 5915	BY4741; *MATa his3Δ1 leu2Δ0 met15Δ0 ura3Δ0 grx2::kanMX4 ade1::URA3*	This study
ABC 5916	BY4741; *MATa his3Δ1 leu2Δ0 met15Δ0 ura3Δ0 grx3::kanMX4 ade1::URA3*	This study
ABC 5917	BY4741; *MATa his3Δ1 leu2Δ0 met15Δ0 ura3Δ0 grx4::kanMX4 ade1::URA3*	This study
ABC 5918	BY4741; *MATa his3Δ1 leu2Δ0 met15Δ0 ura3Δ0 grx5::kanMX4 ade1::URA3*	This study
ABC 5919	BY4741; *MATa his3Δ1 leu2Δ0 met15Δ0 ura3Δ0 grx6::kanMX4 ade1::URA3*	This study
ABC 5920	BY4741; *MATa his3Δ1 leu2Δ0 met15Δ0 ura3Δ0 grx7::kanMX4 ade1::URA3*	This study
ABC 5921	BY4741; *MATa his3Δ1 leu2Δ0 met15Δ0 ura3Δ0 trx1::kanMX4 ade1::URA3*	This study
ABC 5922	BY4741; *MATa his3Δ1 leu2Δ0 met15Δ0 ura3Δ0 trx2::kanMX4 ade1::URA3*	This study
ABC 5923	BY4741; *MATa his3Δ1 leu2Δ0 met15Δ0 ura3Δ0 trx3::*kanMX4 *ade1::URA3*	This study
ABC 5924	BY4741; *MATa his3Δ1 leu2Δ0 met15Δ0 ura3Δ0 prx1::kanMX4 ade1::URA3*	This study
ABC 5925	BY4741; *MATa his3Δ1 leu2Δ0 met15Δ0 ura3Δ0 srx1::kanMX4 ade1::URA3*	This study
ABC 5926	BY4741; *MATa his3Δ1 leu2Δ0 met15Δ0 ura3Δ0 gto1::kanMX4 ade1::URA3*	This study

ABC 5927	BY4741; *MATa his3Δ1 leu2Δ0 met15Δ0 ura3Δ0 gto2::kanMX4 ade1::URA3*	This study
ABC 5928	BY4741; *MATa his3Δ1 leu2Δ0 met15Δ0 ura3Δ0 gto3::kanMX4 ade1::URA3*	This study
ABC 5929	BY4741; *MATa his3Δ1 leu2Δ0 met15Δ0 ura3Δ0 gtt1::kanMX4 ade1::URA3*	This study
ABC 5930	BY4741; *MATa his3Δ1 leu2Δ0 met15Δ0 ura3Δ0 gtt2::kanMX4 ade1::URA3*	This study
ABC 5931	BY4741; *MATa his3Δ1 leu2Δ0 met15Δ0 ura3Δ0 lap1::kanMX4 ade1::URA3*	This study
ABC 5932	BY4741; *MATa his3Δ1 leu2Δ0 met15Δ0 ura3Δ0 lap2::kanMX4 ade1::URA3*	This study
ABC 5933	BY4741; *MATa his3Δ1 leu2Δ0 met15Δ0 ura3Δ0 lap3::kanMX4 ade1::URA3*	This study
ABC 5934	BY4741; *MATa his3Δ1 leu2Δ0 met15Δ0 ura3Δ0 lap4::kanMX4 ade1::URA3*	This study
ABC 5935	BY4741; *MATa his3Δ1 leu2Δ0 met15Δ0 ura3Δ0 aap1::kanMX4 ade1::URA3*	This study
ABC 5936	BY4741; *MATa his3Δ1 leu2Δ0 met15Δ0 ura3Δ0 ecm38::kanMX4 ade1::URA3*	This study
ABC 5937	BY4741; *MATa his3Δ1 leu2Δ0 met15Δ0 ura3Δ0 kex1::kanMX4 ade1::URA3*	This study
ABC 5938	BY4741; *MATa his3Δ1 leu2Δ0 met15Δ0 ura3Δ0 pep4::kanMX4 ade1::URA3*	This study
ABC 5939	BY4741; *MATa his3Δ1 leu2Δ0 met15Δ0 ura3Δ0 cps1::kanMX4 ade1::URA3*	This study

ABC 5940	BY4741; *MATa his3Δ1 leu2Δ0 met15Δ0 ura3Δ0 prc1::kanMX4 ade1::URA3*	This study
ABC 5941	BY4741; *MATa his3Δ1 leu2Δ0 met15Δ0 ura3Δ0 ynl045::kanMX4 ade1::URA3*	This study
ABC 5942	BY4741; *MATa his3Δ1 leu2Δ0 met15Δ0 ura3Δ0 ybr139::kanMX4 ade1::URA3*	This study

Table 2.2: List of plasmids used in the study

Plasmid name	**Clone no.**	**Description**
Vectors		
p416TEF	ABE 443	The CEN-vector bearing URA3 marker and TEF Promoter-MCS-terminator for yeast expression and Amp^r marker for selection in *E.coli*. (Mumberg, et al., 1995)
pRS316	ABE 931	*URA3* marker based yeast centromeric expression vector and Amp^r marker for selection in *E.coli.*
pET23a(+)	ABE 991	This plasmid was procured from Novagen
pRS313	ABE 135	*HIS3* marker based yeast centromeric expression vector and Amp^r marker for selection in *E.coli.*
Plasmids constructed during the study		
p313TEF-GSTM3	ABE5804	The plasmid contains GSTM3 gene (PCR amplified from genomic DNA) at XbaI and EcoR1 sites of p313TEF vector; confirmed by restriction digestion and sequencing.
p416TEF-GRX4	ABE5881	GRX4 gene along with 800bp upstream region was PCR amplified from genomic DNA and cloned at Sal1 and BamHI sites of pRS416 vector; confirmed by restriction digestion and sequencing.

p415TEF-ECM38	ABE5882	ECM38 gene along with its 800bp upstream region was PCR amplified from genomic DNA and cloned at XbaI and XhoI sites of pRS415 vector; confirmed by restriction digestion and sequencing.
pET23a(+)-GSTM3-6X His	ABE5883	GSTM3 gene with C-terminal 6X His tag cloned at NdeI and EcoRI sites of pET23a(+). The clone was confirmed by restriction digestion and sequencing.
pET23a(+)-6X His-GRX4	ABE5884	GRX4 gene with N-terminal 6X His tag cloned at Sal1 and XhoI sites of pET23a(+). The clone was confirmed by restriction digestion and sequencing.

2.3. Oligonucleotides

The list of various oligonucleotide primers used in this study is given in Table 2.3.

Table 2.3: List of Oligonucleotides (and their sequences) used in this study

Oligonucleotide name	**Sequence (5' to 3')**
EcoR1-GSTM3 For.	ATCGCTCTAGAATGGGGGAAAAAAGGACAATAATCAAAGCGC
GSTM3-XbaI Rev.	ATCCGCTCGAGTTAGCTACTGCAGGAAGCTTGCATCATAAAC
GSTM3-6X His-NdeI Rev.	GATGGCTACTGCAGGAAGCTTGCATCATAAAC
EcoR1-6X His-GSTM3 For.	CATGATGGGGGAAAAAAGGACAATAATC
*ade1::*URA3 disruption cassette For.	ATCGCCATATGATGCATCATCACCATCA
*ade1::*URA3 disruption cassette Rev.	AGCCATTACTGCTTTCGCAAAACGC

*ade2::*HIS3 disruption cassette For.	ATGACACAGCGAAGAGATATTCG
*ade2::*HIS3 disruption cassette Rev.	CCAAATTAAACTCATCAAGTGCG
BamH1-Grx4 For.	ATCCGCTCGAGTTAGTGATGGTGATGAT
Grx4-SalI Rev	ATCGCCATATGATCCATCACCGCATCAA
SalI-6X His-Grx4 For.	CCATCCCACATGGGCTCATTTTGC
Grx4-6X His-XhoI Rev.	GTTTCGCAGGGATGATTGCCAACAA
TEF For. (sequencing)	TTGATATTTAAGTTAATAAACGG
TEF Rev. (sequencing)	TTCAGGTTGTCTAACTCCTTC
T7 For. (sequencing)	TAATACGACTCACTATAGGG
T7 Rev. (sequencing)	GCTAGTTATTGCTCAGCGG

2.4 Media

All the media, buffers and stock solutions were prepared using Millipore elix 5 deionized water unless otherwise mentioned. They were sterilized, as recommended, either by autoclaving at 15 lb/inch^2 (psi) pressures at 121ºC for 15 minutes, or by using membrane filters (Advanced Microdevices Pvt. Ltd., India) of pore size 0.2-0.45 µm (for heat labile compounds). Additional amino acid and nutrients were prepared as sterile stock and added as per requirements. Agar was added, if required, at a final concentration of 2.2%. Ampicillin was added at a final concentration of 100µg/mL. Chloramphenicol was added at a final concentration of 25µg/mL.

2.4.1. LB Medium (Luria–Bertani) (per 1000 mL)	Yeast extract 5 g/L Tryptone 10 g/L NaCl 10 g/L [pH was adjusted to 7.0 with 1N NaOH]
2.4.2. YPD Medium (Yeast extract Peptone Dextrose) (per 1000 mL)	Yeast extract 10 g/L Peptone 20 g/L Dextrose 20 g/L
2.4.3 SD Medium (Synthetic Defined) (per 1000 mL)	YNB(Yeast Nitrogen Base) 1.7 g/L (without amino acids and ammonium sulphate) $(NH_4)_2 SO_4$ 5 g/L Dextrose 20 g/L Amino acids (as required) 80 mg/L [pH was adjusted to 6.0–6.5]

2.5 BUFFERS AND STOCK SOLUTIONS

2.5.1 Ampicillin (100 mg/mL) and Chloramphenicol (25 mg/mL) stock solutions

The required amount of ampicillin (sodium salt) was dissolved in the required volume of deionized water, and was filter-sterilized using 0.2μm membrane filter.

Chloramphenicol was dissolved in absolute ethanol and filter-sterilized. Both solutions were stored at -20° C.

2.5.2 Glutathione Stock Solution (100mM)

The required amount of glutathione (reduced form) was dissolved in 10 mL of deionized water and was filter-sterilized using 0.2μm membrane filter. It was stored at -20°C in aliquots.

2.5.3 50% Glycerol (used for preparing –80°C stocks of *E. coli*)

50 mL glycerol is dissolved in 50 mL of deionized water and mixed properly. The solution was autoclaved and stored at room temperature.

2.5.3 25% Glycerol (used for preparing –80°C stocks of *S. cerevisiae*)

2.5.4 IPTG (Isopropyl β-D-1-thiogalactopyranoside) stock solution (500mM)

1.19 g of IPTG is dissolved in 8 mL of distilled H_2O. Bring to a final volume of 10 mL with molecular biology grade H_2O. Filter sterilize with a 0.22μm syringe filter.

2.5.5 Alkaline Lysis Buffers (Plasmid DNA preparation from *E. coli*)

a) Solution-I (Resuspension Solution)	50 mM Glucose 25 mM Tris-HCl (pH 8.0) 10 mM EDTA (pH 8.0) Autoclaved and stored at 4ºC.
b) Solution-II (Lysis Solution) (freshly prepared)	0.2N NaOH (freshly diluted from a 10N stock) 1% SDS (freshly diluted from a 10% stock) Stored at room temperature.
c) Solution-III (Neutralization Solution)	5M Potassium acetate 60 mL Glacial acetic acid 11.5 mL Deionized water 28.5 mL The resulting solution is 3M with respect to potassium and 5M with respect to acetate. It was stored at 4ºC.
d) TE Buffer (Tris-EDTA) (pH 8.0)	10 mM Tris-HCl (pH 8.0). 1 mM EDTA (pH 8.0).
e) TE-RNAse (stock 10 mg/mL)	Working stock 20 μg/mL in TE Buffer, pH 8.0.

2.5.6 Agarose Gel Electrophoresis Reagents

a) 1× TAE (Tris-acetate-EDTA) Buffer (per 1000 mL) **(prepared from 50× TAE stock)**	40 mM Tris-acetate. 1mM EDTA (pH 8.0). Autoclaved and stored at room temperature.
b) Orange-G dye (Gel loading dye, 6X)	0.25% orange-G 30% glycerol
c) 0.7-1% Agarose gel in 1× TAE	
d) Ethidium Bromide (10 mg/mL) Stock	Final working concentration used at 0.5µg/mL.

2.5.7 Solutions for preparation of chemical competent *E. coli* cells

a) SOB	Bactotryptone 20 g Bacto yeast extract 5 g NaCl 0.5 g Above mentioned components were dissolved in 950 mL of water. 10 mL of 250 mM KCl was added and pH was adjusted to 7 with 5N NaOH, volume was made up to 995 mL and autoclaved. Just before use, 5 mL of filter sterilized 2 M $MgCl_2$ was added.
b) SOC	SOB + 20 mM Glucose
c) 10% glycerol	

2.5.8 Yeast Transformation Solutions (*S. cerevisiae*) [31]

a) 0.1M Lithium acetate in TE (pH 7.5)

b) 50% PEG-3350 in 0.1 M Lithium acetate in TE (pH 7.5).

2.5.9 Breaking buffer for genomic DNA isolation from yeast

10 mM Tris-HCl (pH 8.0)

1 mM EDTA (pH 8.0)

100 mM NaCl

1% (w/v) SDS

2% (v/v) Triton X-100

2.5.10 SDS-PAGE Solutions and Reagents

a) 30% Acrylamide Mix	29.2% (w/v) acrylamide 0.8% (w/v) N, N'- methylenebisacrylamide Filtered before use.
b) Resolving (Lower) Gel Tris Buffer (Stock) (4×) 1.5 M Tris-HCl (pH 8.8)	18.18 g Tris pH adjusted to 8.8 with 6N HCl and volume made up to 100 mL. (0.4% SDS can be added to the buffer itself).
c) Stacking (Upper) Gel Tris Buffer (Stock) 0.5 M Tris-HCl (pH 6.8)	6.06 g Tris pH adjusted to 6.8 with HCl and volume made up to 100 ml. (0.4% SDS can be added to the buffer itself).
d) 0.4% SDS	
e) TEMED	
f) APS (Ammonium persulphate)	10%
g) Tris-Glycine Gel Running Buffer (Laemmli Buffer) (pH 8.3)	25 mM Tris base 250 mM Glycine (electrophoresis grade) 0.1% SDS
h) 2× SDS Gel Loading Buffer (pH 6.8)	100 mM Tris-HCl (pH 6.8)

	4% (w/v) SDS 20% (v/v) Glycerol 200 mM β-mercaptoethanol (add immediately before use) 0.2% (w/v) Bromophenol blue
i) Gel Staining Solution	40% (v/v) Methanol 10% (v/v) Glacial Acetic acid 50% (v/v) Distilled water 0.1% Coomassie Brilliant Blue (R250)
j) Gel Destaining Solution	40% (v/v) Methanol 10% (v/v) Glacial Acetic acid 50% (v/v) Distilled water

Composition of SDS-PAGE Resolving (Lower) Gel (10%) (For 5 mL)

a)	Distilled water	1.9 mL
b)	Resolving (Lower) Gel Tris Buffer (Stock) (4×) 1.5 M Tris-HCl (pH 8.8)	1.3 mL
c)	30% Acrylamide Mix	1.7 mL
d)	10% SDS	0.05 mL
e)	10% APS (Ammonium persulphate)	0.05 mL
f)	TEMED (N, N, N', N'-Tetramethylethylenediamine)	0.01 mL

Composition of SDS-PAGE Stacking (Upper) Gel (5%) (For 3 mL)

a)	Distilled water	2.1 mL
b)	Stacking (Upper) Gel Tris Buffer (Stock) 1M Tris-HCl (pH 6.8)	0.38 mL
c)	30% Acrylamide Mix	1.5 mL
d)	10% SDS	0.03mL
e)	10% APS (Ammonium persulphate)	0.03mL
f)	TEMED (N, N, N', N'-Tetramethylethylenediamine)	0.003 mL

2.5.11 Immunoblotting (Western Blotting) Reagents

a) Transfer Buffer (pH 9.2)	48 mM Tris base 39 mM Glycine 0.037% SDS 20% Methanol
b) Tris-Buffered Saline (TBS)	150 mM NaCl 20 mM Tris-HCl (pH 7.5) (Made as 10× stock and kept at 4°C)
c) Washing Buffer **TBS-Tween 20 (TBST) Buffer**	0.1% Tween 20 in TBS (pH 7.5)
d) Blocking Agent	5% Skim milk in TBST.

SECTION B: METHODS

2.6 Growth and maintenance of bacteria and yeast strains

The *Escherichia coli* DH5〈 strains were routinely grown in LB medium at 37°C. *E. coli* transformants were selected and maintained on LB medium supplemented with ampicillin.

The *Saccharomyces cerevisiae* strains were regularly maintained on YPD medium and grown at 28-30°C. The yeast transformants were selected and maintained on SD medium with amino acid supplements as per requirements.

2.7 Recombinant DNA methodology (restriction digestion, ligation, transformation of *E. coli.* PCR amplification, etc)

All the molecular techniques used in the study for manipulation of DNA, protein, bacteria and yeast were according to standard protocols [19,23] or as per manufacturer's protocol, unless specifically mentioned. DNA sequencing was done using FIRST BASE sequencing services.

2.8 Transformation of yeast

The transformation of *S. cerevisiae* strains was carried out by lithium acetate method [31]. *S. cerevisiae* cultures were grown in YPD at 30⏐C with shaking for 16-24 hrs and then reinoculated in fresh YPD to an initial OD_{600} of 0.1, cells were allowed to grow at 30⏐C for 4-5 hrs with shaking. Cells were harvested at 6000 rpm for 5 min, then were washed with sterile water followed by subsequent wash with 0.1M lithium acetate solution (prepared in TE, pH 7.5) and were finally resuspended in the same solution. The cells were spun down, suspended in 0.1 M lithium acetate solution to a cell density of $1 \cdot 10^9$ cells/mL and divided into 100⎡L aliquots. Approximately 50 ⎡g (5⎡L of 10 mg/mL stock solution) of heat denatured, salmon sperm carrier DNA, 0.3⎡g- 0.7⎡g of plasmid/DNA fragment and 0.3mL of 50% PEG 3350 (prepared in 0.1M lithium acetate, pH 7.5) were added to each aliquot and whole cell suspension was subjected to heat shock at 42⏐C for 30 min. The cell suspensions were allowed to cool to room temperature. The cells were centrifuged at 9000 rpm for 5 min. The cell pellet was resuspended in sterile water and appropriate volume of cell suspension was plated on selection plates.

2.9 Construction of *ade1/ade2::*URA/HIS disruption cassette

The *ade1/ade2*::URA/HIS disruption cassette were excised by PCR with respective primers from pRS313 and pRS416 followed by agarose gel electrophoresis and elution of the required band.

2.10 Construction of yeast strains used in the study: disruption of ADE1/ADE2 gene in different *S. cerevisiae* gene deletion strains

The ADE1/ADE2 ORF was disrupted in different *S. cerevisiae* gene deletion strains using the *ade1/ade2::URA/HIS* disruption cassette. The disruption cassette was constructed and excised as explained in section 2.7. The different *S. cerevisiae* deletion strains were transformed with this disruption cassette and selected on minimal media lacking histidine and uracil. Only transformants with specific insertion of cassette were used for color assay by dilution spotting.

2.11 Isolation of genomic DNA from yeast

Genomic DNA from *S. cerevisiae* strains was isolated as described in [2] using the glass bead lysis method and the Breaking buffer, described in section 2.5.9.

2.12 Growth assay by dilution spotting

For dilution spotting yeast cells were grown in selective minimal medium. Primary cultures were grown for 12-16 hours at 30°C, with shaking at 200 rpm. Primary cultures were used to inoculate a secondary culture in selective minimal medium for 8 hours or till OD_{600} reaches between 0.6-0.8 at 30°C. Cells were centrifuged , washed with sterile water and resuspended into sterile water at OD_{600}= 0.2.

Four serial dilutions were made in sterile water; $O.D_{600}$= 0.2, 0.02, 0.002, 0.0002. 10µl of each of these cell suspensions were spotted on the selective minimal medium plates. Plates were incubated at 30°C for 2-5 days and photographs were taken.

2.13 Recombinant expression and purification of His-tagged GSTM3 and Grx4 protein in *E. coli*

pET23a(+)-6X His-GSTM3 and pET23a(+)-6X His-Grx4 (ABE 5369) was transformed in BL21 and transformants were selected on LB+Amp plates. The primary culture was grown overnight in LB media containing antibiotics- 100µg/ml ampicillin for selection. The secondary culture was inoculated at 0.05 $O.D_{600}$ and allowed to grow until $O.D_{600}$ reached 0.6-0.8. The culture was induced using 1mM IPTG and kept at 18ºC for 18 hrs at 200rpm.

The cells were harvested by centrifugation at 2500g for 10 min at 4ºC. The cells were lysed by sonication using lysis buffer, pH 7.4 (50mM Sodium phosphate monobasic, 300mM NaCl, 5mM imidazole and 1mM PMSF) with 10sec on and 15sec off cycle and 20% amplitude. The cell lysate was centrifuged at 10000 rpm for 30 min. at 4°C. The supernatant obtained was incubated with washed Ni-NTA beads for 1 hr at 4°C. The supernatant-bead slurry was centrifuged at 270g, 4°C; the supernatant was aspirated and protein-bound beads were collected. Beads were subjected to three washes (centrifuged at 800g, 4°C with wash buffer containing 50mM Sodium phosphate monobasic, 300mM NaCl, 20mM imidazole and 1mM PMSF. The specific protein bound to beads was eluted in elution buffer containing 50mM Sodium phosphate monobasic, 300mM NaCl, 250mM imidazole and 1mM PMSF by centrifugation at 800g, 4°C followed by collection of eluate which contains specific protein of interest. The protein fractions obtained were run on 10% SDS-PAGE to check the purity of the protein. Dialysis was performed (using Thermo Scientific 3.5K MWCO dialysis tubing) to remove imidazole by buffer exchange with dialysis buffer (50mM Sodium phosphate monobasic and 300mM NaCl). After dialysis the protein concentration was estimated using NanoDrop. The protein was flash-frozen in liquid nitrogen and stored at -80°C.

2.14 Protein concentration and quantification

The concentration of protein in the samples was estimated using Bradford reagent as per the manufacturer's instructions. The protein samples were diluted 20 times and 2.5µl of each diluted sample was used for protein estimation, BSA (Albumin, Fraction V, USB Cat # 70195) used as standard. Protein estimation was also carried out by scanning the protein at A280 and concentration was calculated using the extension coefficient of protein. The estimation were done in triplicates.

2.15 Gel filtration analysis of proteins

Gel filtration was carried out for further purification and to determine the oligomeric status of the proteins. The active fractions eluted from the Ni-NTA column were loaded onto a size exclusion gel filtration column Superdex 200 10/300 GL and gel filtration was performed using 50mM Tris and 300mM NaCl buffer (pH-8). Molecular weight determinations were done after calibration.

2.16 Western blot analysis of C-terminal HA tagged GSTM3

Equal amount of protein samples were loaded on a 10% SDS–polyacrylamide gel, along with Goldbiotech pre-stained ladder. The gel was run at 120V.The gel was electro-blotted onto Hybond ECL nitrocellulose membrane (Amersham Bioscience) at 90V for 1.5 hrs using Tris-glycine transfer buffer. Immediately after the transfer, the membrane was incubated at for 3 hrs in blocking buffer (5% skim milk in TBST buffer). After blocking the membrane it was probed with rabbit anti-his primary antibody at a dilution of 1:4000 in blocking buffer for 1 hr at room temperature. After 3×15 minutes washing of the blot with TBST, the membrane blot was incubated for 1 hr in anti-mouse (horseradish peroxidase-conjugated) antibody at a dilution of 1: 8000 in blocking buffer. After 3×15 minutes washing of the blot with TBST, the blot was sprayed with chemiluminescent HRP substrate. The signal was detected in LAS Imaging System.

2.17 Extraction of Felinine and Sample preparation for HPLC

Extraction of Felinine was carried out as described earlier (Chemistry & Biology 13, 1071–1079, October 2006) with some modifications. Essentially, *Saccharomyces cerevisiae* cells were grown in 100 mL SD media supplemented with appropriate amino acids and grown at 30 °C with shaking (250 rpm). After two days, the cells were harvested and washed with deionized water and kept at −20 °C. To the frozen pellet, 3 mL of Dimethyl sulphoxide (DMSO) was added, then vortexed for 1 min and incubated at 55 °C in the water bath for 1h. 1g 0.50–0.75mm glass beads were added, and the cells were broken using a glass bead beater. The cells were centrifuged to remove cell debris. Acetone was added to the pellet, vortexed, and centrifuged. This process was repeated till the pellet became colorless. The acetone and DMSO fractions were mixed with an equal amount of Hexane, which was collected after separation of the two layers. The hexane layer was washed with distilled water and then with brine solution twice.

The solvent was evaporated under a rotary evaporator (till dry) in dim light and was dissolved in 1 mL acetonitrile:trifluroacetic acid:water (10:0.1:89.9 v/v) for analysis by high performance liquid chromatography (HPLC). HPLC separation and quantification was performed on a Waters System using C18 − 5µm intersil ODS-P, 250×4.6mm column (LCGC) using the solvent acetonitrile:trifluroacetic acid:water (10:0.1:89.9 v/v) with flow rate 0.3 mL/min at 32 °C.

2.18 Mass spectrometry analysis of the purified Felinine

The purified felinine was subjected to mass spectrometric analysis to confirm the formation of felinine in the recombinant yeast. The felinine mass was analyzed using WATERS SYNAPT G2S QTOF mass spectrometer in TOF MS ES+ mode. The mass range and scan rate were set to record m/z from 160 to 420 m/z in resolution mode. The sample was directly infused with a flow rate of 100µl/min. Raw data obtained was analyzed using MassLynx software.

2.19 Enzyme Assay and Kinetics

The Glutathione S-Transferase (GST) Assay Kit utilizes 1-Chloro-2,4-dinitrobenzene (CDNB) which is suitable for the broadest range of GST isozymes. Upon conjugation of the thiol group of glutathione to the CDNB substrate, there is an increase in the absorbance at 340 nm.

A. Assay in 1 ml quartz cuvette

1. Prepare a 10-ml reaction master mix, which is sufficient for 10 assays when a 1 ml quartz cuvette is used (Option A1). The solution must be freshly prepared for each assay series and should be used within 60 minutes of preparation. Alternatively, individual reactions can be prepared for 1-ml cuvettes (Option A2).

Reagent Option A1 Option A2 Dulbecco's Phosphate Buffered Saline 9.8 ml 980 ml 200 mM L-Glutathione reduced 0.1 ml 10 ml 100 mM CDNB 0.1 ml 10 ml The solution might become slightly cloudy upon the addition of CDNB to the solution. This cloudiness disappears when the solution is completely mixed.

2. Set the spectrophotometer at 340 nm. On a kinetic program: read every 30 seconds over a period of 5 minutes after a lag time of 1 minute.

3. Transfer 1 ml of the substrate solution to a quartz cuvette and read the Blank absorbance at 340 nm

4. Add 2-50 ml GST sample or 2 ml of the GST control, provided with the kit, directly to the quartz cuvette containing up to 1 ml substrate solution. Mix by covering the cuvette with a parafilm and inverting several times. Note: The sample should be read as close as possible to the addition of the GST enzyme (sample or control).

5. Record the absorbance readings according to the kinetics program described above. (Note: If the GST control or GST sample is too concentrated, it must be diluted with Sample Buffer prior to the assay. The dilution factor must be determined experimentally).

The increase in absorbance is directly proportional to the GST activity. The linearity of the reaction must be determined by plotting the absorbance values against time. Calculate the change in absorbance (ΔA_{340})/minute, in the linear range of the plot, for the sample and for the blank using the following equation:

$$(\Delta A_{340})/\text{min} = A_{340}(\text{final read}) - A_{340}(\text{initial read}) / \text{reaction time (min.)}$$

Subtract the (ΔA_{340})/minute of the blank from the (ΔA_{340})/minute of the sample. Use this rate for the calculation of the GST specific activity. Note: For measurements in 1 ml cuvettes, the initial reading is the first reading after the lag time (1 minute). Calculate the GST activity using the following equation:

GST specific activity:

$$(\Delta A_{340})/\text{ min x V (ml) x dil } /(\varepsilon_{mM} \text{ x } V_{enz} \text{ (ml)}) = \mu\text{mol/ml/ min}$$

Where: dil = the dilution factor of the original sample ε mM (mM^{-1} cm^{-1}) - the extinction coefficient for CDNB conjugate at 340 nm.

2.20 Sequence analysis

Protein sequences were retrieved from NCBI and UniProt database and multiple sequence alignment was done using Clustal omega server. JalView software was used for visualization purpose. Protein structures were retrieved from PDB database, structure was predicted using iTASSER server (Y Zang, 2008). For structural alignment of proteins, Pymol software was used.

Chapter 3: The ade pigmentation of yeast: Uncovering the missing glutathione-S-transferase in the pathway

3.1.1 Introduction

The glutathione-mediated pathway for the detoxification of endogenously and exogenously derived toxic compounds has been investigated in detail using a pigment that accumulates in certain adenine biosynthetic mutants of yeasts by K. G. Sharma *et al.*, 2003; B. Chaudhuri *et al.*, 1997 and it is known that the ade1 / ade2 mutants of *Saccharomyces cerevisiae*, when grown on adenine-limiting medium, accumulate a characteristic red pigment (ade pigment) in their vacuoles(10). The precursors of these ade pigments are toxic intermediates of the adenine biosynthetic pathway (phosphoribosylaminoimidazole (AIR) and phosphoribosylaminoimidazole carboxylate (CAIR)). These intermediates that form conjugates with glutathione, these conjugates are then transported into the vacuole. Further , this red pigment phenotype used as a phenotypic screen to obtain insight regarding new genes involved in the three phases of this detoxification pathway: the activation phase (phase I), the conjugation phase (phase II), and the efflux phase (phase III)(16). Figure 3.1 gives a diagrammatic representation of the ade pathway in *Saccharomyces cerevisiae* and the process by which ade intermediates could be removed by detoxification.

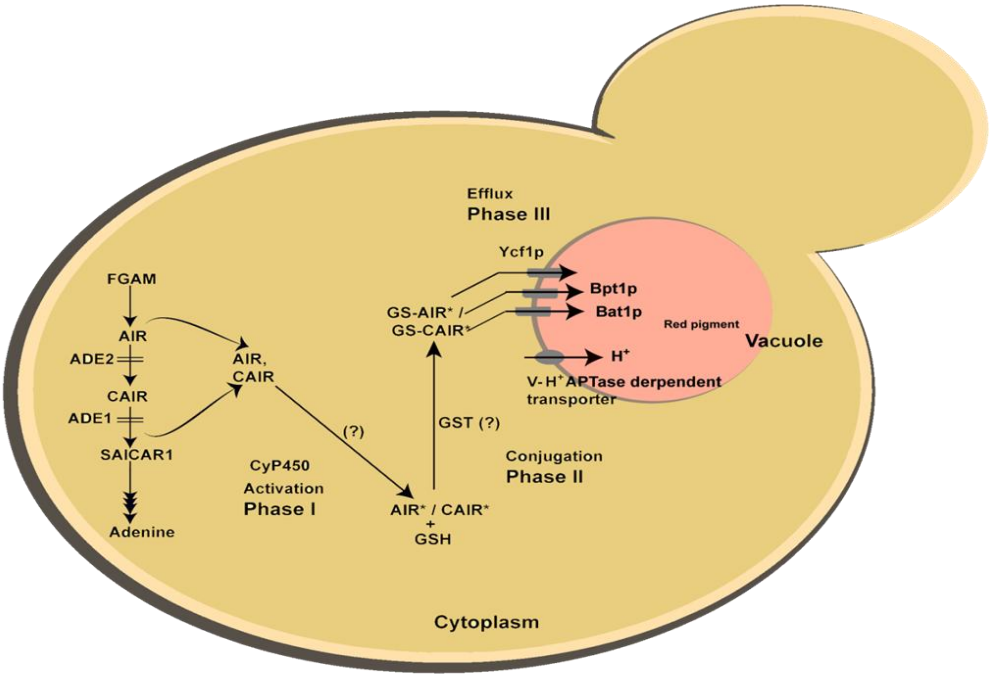

Figure 3.1: The ade intermediate detoxification pathway (Figure reproduced from Sharma *et al*., 2003)

3.1.2 A detailed description of the ADE pathway in *S. cerevisiae*

As mentioned above, the GSH detoxification pathway typically consists of 3 different phases. In yeasts, the role of the initial activation phase is only predicted and yet to be deciphered. Phase 2 on the other hand is a conjugation phase that takes place in the cytosol. This conjugation phase is then followed by the efflux phase.

Previously, it has shown that during the efflux phase, the GSH conjugates are removed from the cytosol in a process controlled by a set of dedicated proteins that belong to the MRP (multidrug associated resistance proteins) sub-family of the family of ABC transporters. This removal in the case of mammalian cells occur by the efflux out of the cell, hence the MRPs are localized on the plasma membrane (Cole et al. 1992; Decottignies and Goffeau 1997; Taglicht and Michaelis 1998). In the case of yeasts and plants the glutathione conjugates are removed from the cytoplasm into the vacuole by similar pumps localized to the vacuole.

3.1.3 'AIR' and 'CAIR' Intermediates in adenine biosynthesis

Phosphoribosylaminoimidazole (AIR) and phosphoribosylaminoimidazole carboxylate (CAIR) are toxic intermediates that accumulate in ade mutants. These toxic intermediates appear to form conjugates with glutathione and which are then transported inside the vacuole through a glutathione conjugate (GS-X) pump (Chaudhuri et. al., 1997). Thus, AIR and CAIR are the precursors to the characteristic red adenine pigmentation. Figure 3.2 gives a schematic of the Adenine biosynthetic pathway. The red pigmentation was an end product in the detoxification of the toxic intermediate that accumulates in vacuole of these mutants.

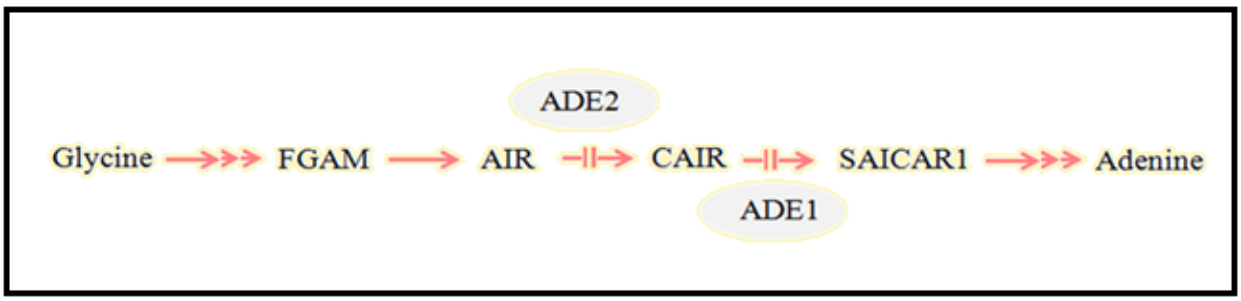

Figure 3.2: A diagrammatic representation of the Adenine Biosynthesis pathway

3.1.4 Transporters involved in the AIR/CAIR detoxification pathway

Previous studies have shown that Ycf1p and Bpt1p (Sharma et. al. 2002), ABC transporters that are a members of the yeast MRP family are primarily involved in glutathione-conjugate transport. Although Ycf1p and Bpt1p are found to be primarily involved in the transport of the glutathione conjugates to the vacuole, deletion of these pumps still revealed residual pigmentation. Further studies then revealed that BAT1 and VPH1, were also involved in the transport of these conjugates.

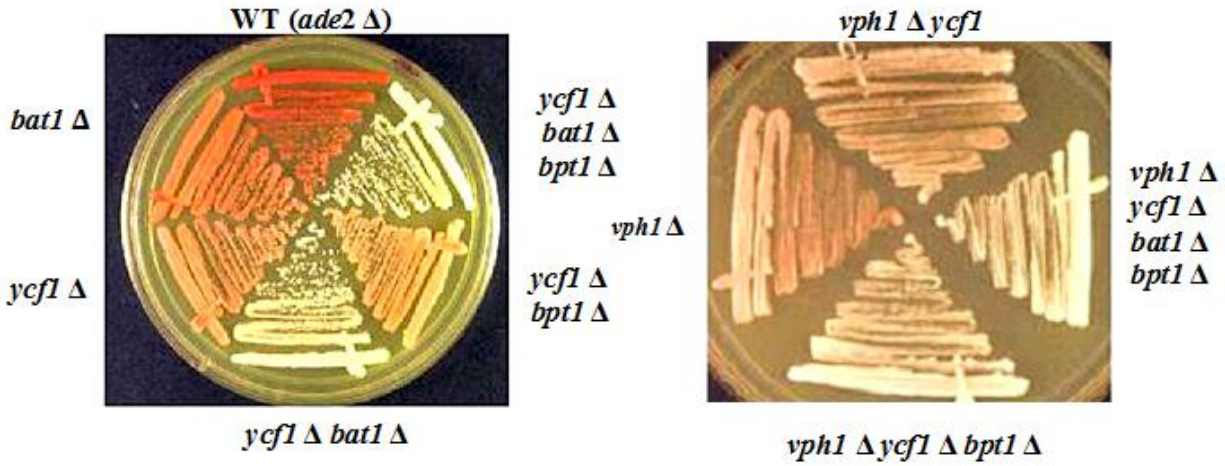

Figure 3.3: The effect of vacuolar pump deletion on pigmentation (Figure reproduced from Sharma *et al*., 2003)

In the triply deleted (*ycf1*Δ*bat1*Δ*bpt1*Δ*vph*Δ) background, the conjugated product (GS-AIR/CAIR) cannot enter the vacuole and hence no red color is observed.

3.1.5 Adenine biosynthesis pathway activation in ade1 / ade2 mutants:

The adenine biosynthesis pathway is derepressed only when the adenine concentration in the cell is below a critical value. In the presence of excess adenine, the biosynthetic pathway is repressed. The ade1/ade2 mutants with excess adenine showed no pigmentation in the cells.

However in limiting adenine levels, the biosynthetic pathway is derepressed. Under such conditions, when the ade1/ade2 genes are deleted, the intermediates (AIR/CAIR) can accumulate and lead to red pigment formation.

3.2 Objective

(1) To identify the putative Glutathione-S-Transferases (GSTs) involved in the conjugation of adenine intermediates, 5′-phosphoribosylaminoimidazole (AIR) / 5′-phosphoribosylaminoimidazole carboxylate (CAIR) to Glutathione and investigates the role of vacuolar enzymes (if any) in the processing of the Glutathione conjugates in the vacuole.

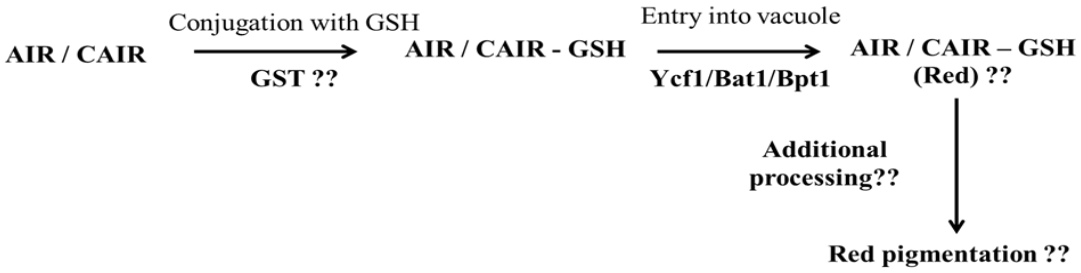

Figure 3.4: A diagrammatic representation of the objective

3.3 Results and Discussion

3.3.1. Identification of Putative GST involved in GS-AIR/CAIR conjugation:

Work with mammalian systems has revealed that members of the thioredoxin superfamily can participate in the conjugation of GSH with different substrates. In order to identify the putative enzymes involved in the conjugation of adenine intermediates, (AIR / CAIR) with Glutathione, the members of yeast thioredoxin superfamily that include GSTs / GST like proteins were first identified. The localizations of these GSTs / GST like proteins are shown in the figure below.

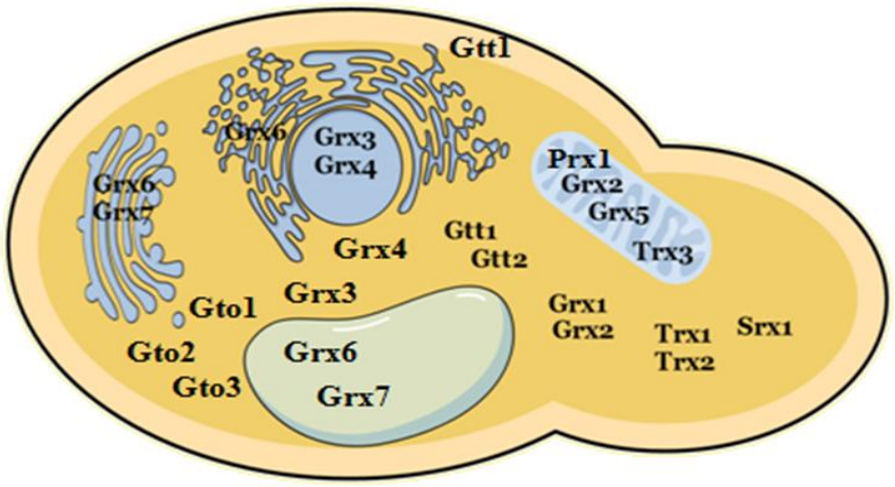

***Fi*gure 3.5**: A schematic representation of different GSTs/GST like proteins found in *Saccharomyces cerevisiae*

S. No.	Gene Name	Protein Family	Localization	Role in glutathionylation and deglutathionylation
1	GTT1	Glutathione-S-Transferase	Endoplasmic Reticulum	Glutathionylation
2	GTT2	Glutathione-S-Transferase	Cytoplasm and Mitochondria	Glutathionylation
3	GRX1	Glutaredoxin	Cytoplasm	Deglutathionylation
4	GRX2	Glutaredoxin	Mitochondria and Nucleus	Deglutathionylation/Glutathionylation
5	GRX3	Glutaredoxin	Cytoplasm and Nucleus	Deglutathionylation/Glutathionylation
6	GRX4	Glutaredoxin	Cytoplasm and Nucleus	Deglutathionylation/Glutathionylation
7	GRX5	Glutaredoxin	Mitochondria	Deglutathionylation/Glutathionylation
8	GRX6	Glutaredoxin	Vacuole	Deglutathionylation/Glutathionylation
9	GRX7	Glutaredoxin	Golgi Apparatus and Vacuole	Deglutathionylation/Glutathionylation
10	TRX1	Thioredoxin	Nucleus, Cytoplasm, Golgi Apparatus and Mitochondria	Deglutathionylation
11	TRX2	Thioredoxin	Nucleus, Cytoplasm and Golgi Apparatus	Deglutathionylation

12	TRX3	Thioredoxin	Mitochondria	Deglutathionylation
13	PRX1	Peroxiredoxin	Mitochondria	Deglutathionylation
14	GTO1	Omega-class GST	Peroxisome	Glutathionylation
15	GTO2	Omega-class GST	Cytoplasm	Glutathionylation
16	GTO3	Omega-class GST	Cytoplasm	Glutathionylation
17	SRX1	Sulfiredoxin	Nucleus and Cytoplasm	Deglutathionylation

Table 3.1: Families, localization and functions of different GSTs/GST like proteins found in Saccharomyces cerevisiae

After identifying the GSTs / GST like proteins and their localizations we procured knockouts of these genes from Euroscarf. We attempted to elucidate their role in ade pigment formation by deleting *ADE1* and *ADE2* genes independently in the different GSTs knockout strains to identify the putative GST involved in the AIR/CAIR conjugation. 17 GSTs / GST like proteins were identified including glutaredoxin family (GRX1, GRX2, GRX3, GRX4, GRX5, GRX6 and GRX7), thioredoxin family (TRX1, TRX2 and TRX3), GSTs (GTT1 and GTT2), sulfiredoxin (SRX1), peroxiredoxin (PRX1), omega class GSTs (GTO1, GTO2 and GTO3). This was done due to the fact that in the absence of the specific GST(s) involved, the red pigmentation would disappear.

PCR-based ADE1::URA3 disruption cassette and ADE2::HIS3 disruption cassette were created to disrupt ADE1 and ADE2 genes separately in different GST knockout strains. The growth of yeast colonies were selected on + adenine and –URA / HIS plates after transforming them with the required disruption cassette. Finally their phenotype was examined to confirm the disruption (adenine auxotroph).

3.3.2. Evaluation of the role of the different thioredoxin superfamily members in the ade pigment formation

As can be seen from the figure below, during excess adenine concentrations all the disruptions are white despite the presence of selecting the ade1 or ade2 deletions, while without adenine no growth is seen as expected since these are adenine auxotroph. Only under limiting adenine conditions (8mg/L)

could the typical ade pigmentation become apparent. The different mutants showed slight variations in color.

(a)

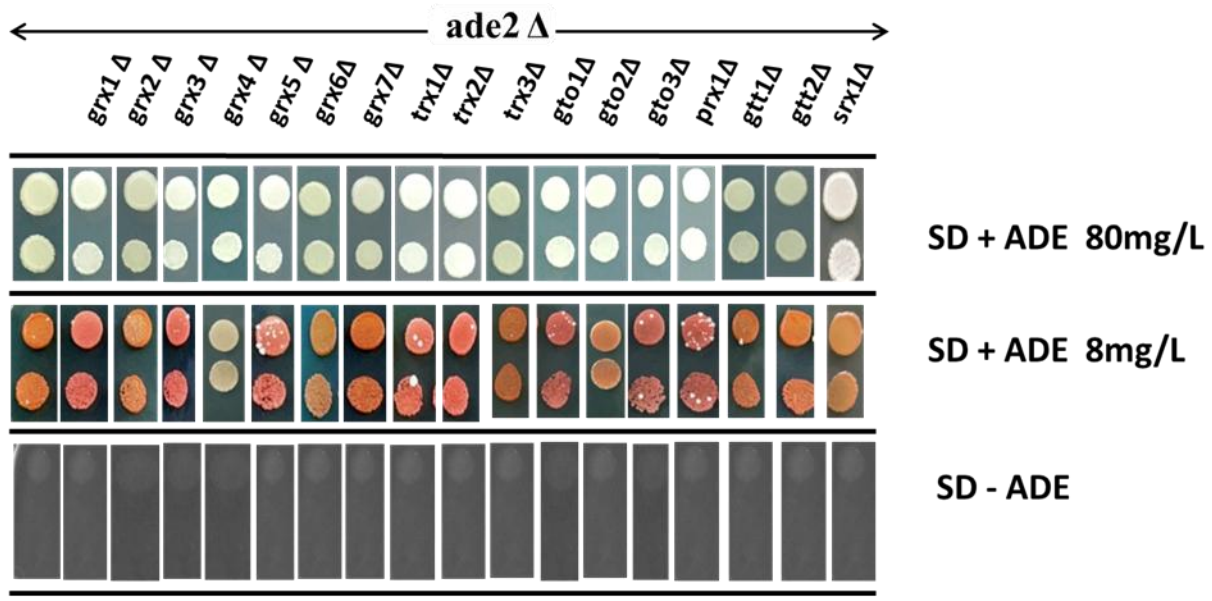

(b)

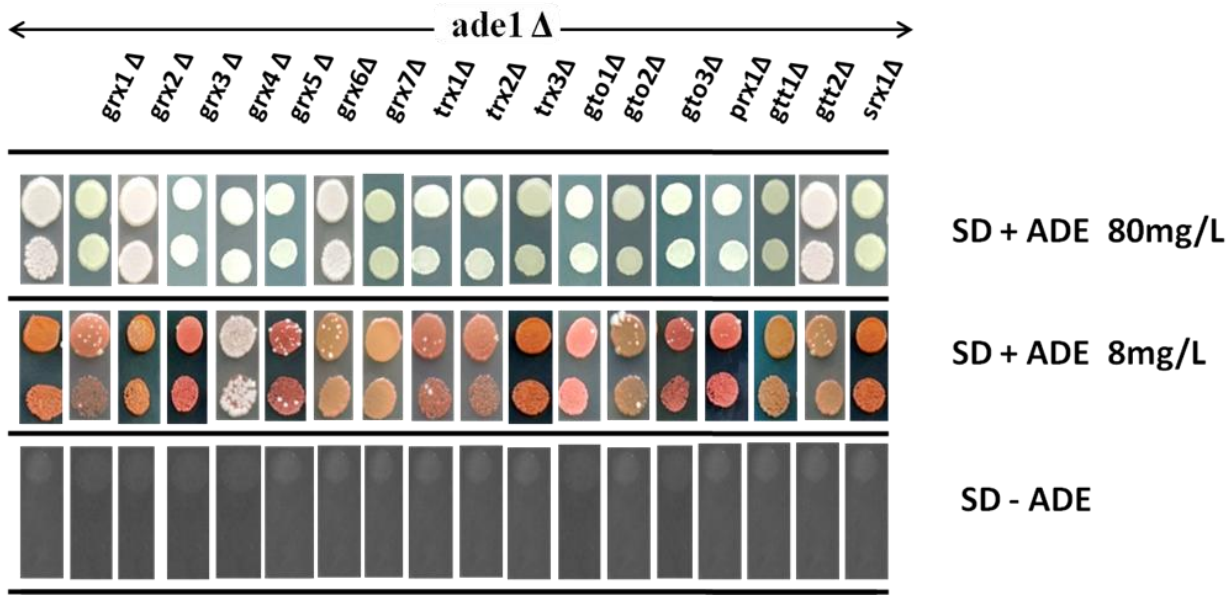

***Fi*gure 3.6**: Pigmentation phenotype of different GSTs upon (a) ade2Δ or (b) ade1Δ in media containing different concentrations of adenine

From figure 3.6, it can be inferred that, in excess adenine supplementation no red pigmentation is observed. Therefore we had a need to maintain a limiting/minimal adenine external environment so that the adenine biosynthetic pathway is activated which will lead to the accumulation of adenine intermediates. There was no growth observed in the SD-ADE plates as these deletion stains were adenine auxotroph. In the case of *grx4Δ* there was no red pigmentation observed both in the ade1Δ and ade2Δ background. The grx4Δ colonies were light pink (almost white) and red color yeast colonies in adenine limiting external environment (8mg/L). All these observations were common to both *ade1Δ* and *ade2Δ*. *grx4Δ* shows almost complete lack of pigmentation in both *ade1Δ* and *ade2Δ* backgrounds.

A few white colored colonies were found amongst the pink or red colored spottings. These were especially consistent in the grx5Δ and prx1Δ backgrounds. Both GRX5 and PRX1 are mitochondrial localized, the white colonies are likely to be petite mutations which spontaneously arise.

3.3.3. Effect of GSH on the red pigmentation

Since many of the members of the thioredoxin superfamily, especially the thioredoxins and glutaredoxins are part of the redox systems of the cell and have both overlapping and participatory functions with GSH. We conjectured that their deletions might divert some of the GSH towards more redox function than detoxification and thus might have an impact on the levels of pigmentation. We thus evaluated these mutants under limiting ade conditions but supplemented with GSH. We observed that almost all the strains which were pink in color became more red when supplemented with GSH. However, in the case of *grx4Δ,* even addition of glutathione did not comport any pigmentation all the double deleted strains were red in color when supplemented with GSH. The studies revealed that the addition of glutathione (GSH) to the medium enhances pigmentation levels (*grx4Δ* still shows absence of pigmentation).

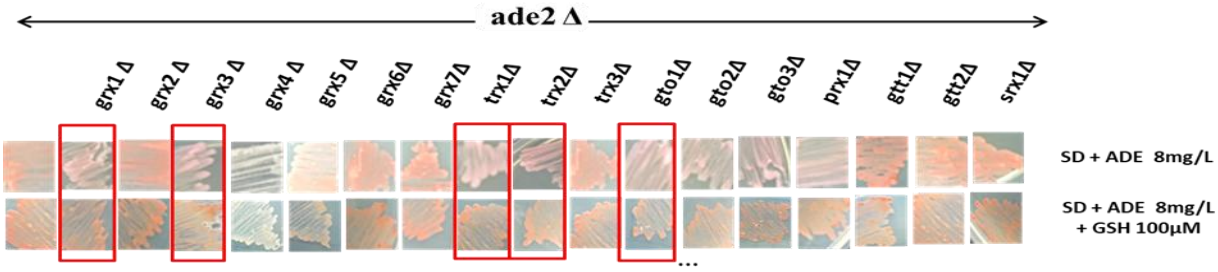

***Fi*gure 3.7**: A Figure showing the effect of GSH and different adenine concentration on the red pigmentation

The results also suggested that the pink coloration could be due to the limiting amount of GSH rather than any cooperative actions of more than one GSTs. Since limiting levels of GSH caused difference in coloration pattern, we were interested to see if a similar observation can be obtained by limiting the concentrations of adenine in the double deleted strain background. A schematic representation of this process is given in figure 3.8.

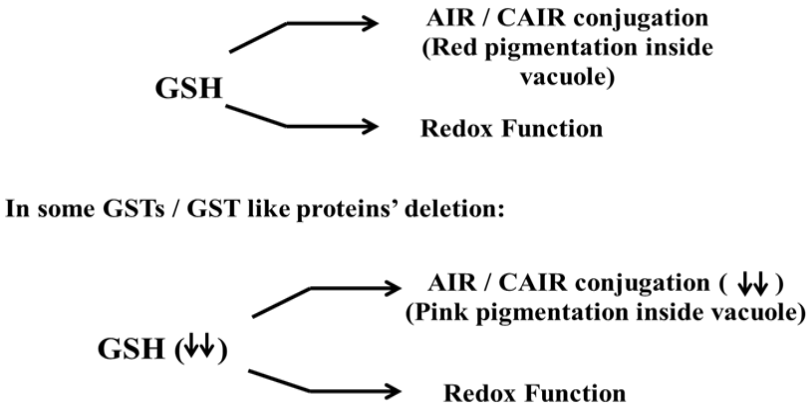

***Fi*gure 3.8**: A schematic showing the effect of GSH concentration on the red pigmentation

3.3.4. Effect of different adenine concentration on growth and red pigmentation

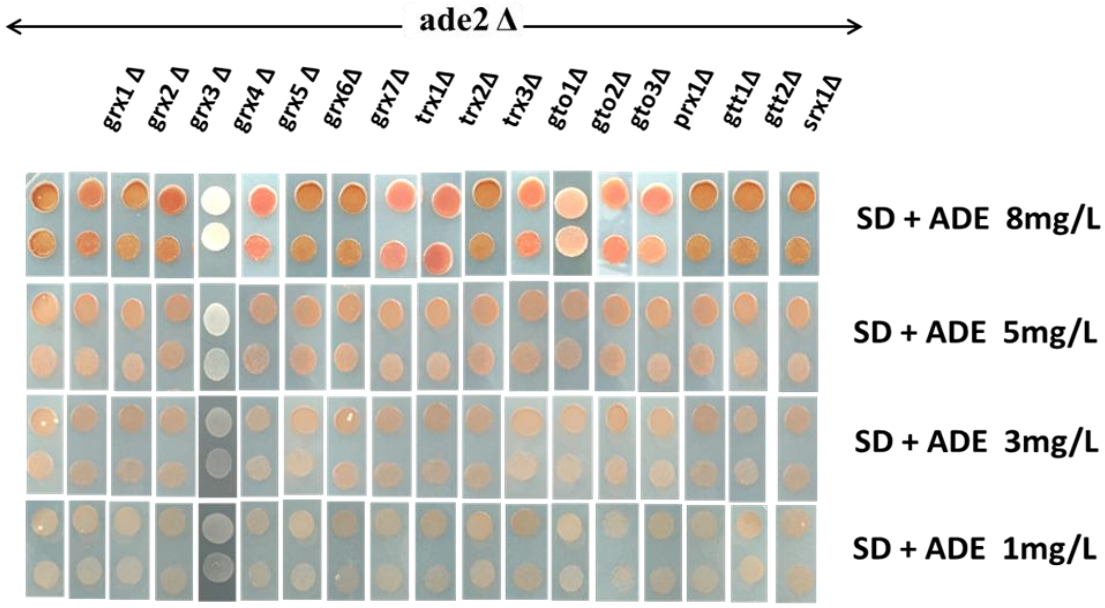

***Fi*gure 3.9**: Figure showing the effect of different adenine concentration on the red pigmentation

We also wished to evaluate how levels of adenine concentrations in the media affected growth and pigmentation. We observed that if the concentration of adenine was brought below 8mg/L, the color difference between the different strains was not observed and further they suffered from growth defect. This growth defect can be accounted by the very minimal levels of adenine.

Thus optimal levels of both the substrates (GSH and AIR/CAIR) are required to obtain the right level of red pigmentation.

3.3.5. Effect of temperature on the red pigmentation

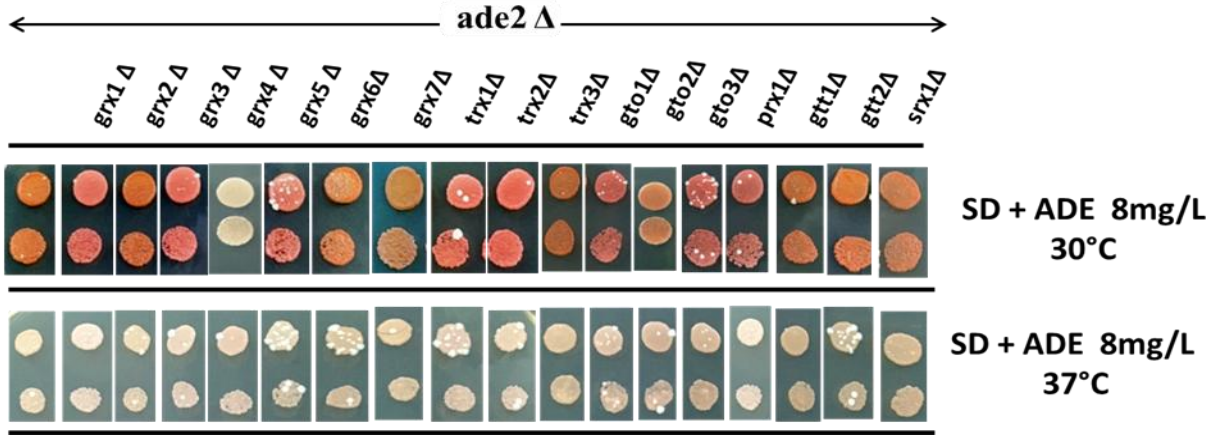

***Fi*gure 3.10**: Effect of temperature on the red pigmentation

Temperature fades pigmentation of the different deletions; grx4Δ stills lacks pigmentation:

Temperature is known to affect the pigmentation levels of ade1/ade2 mutants. We wished to evaluate the level of pigmentation with elevated temperature. Therefore we subjected all the mutants (under limiting adenine condition) to growth at both 30^{o}C and 37^{o}C. We observed significant reduction in pigmentation in all the deletions. The utilization of GSH in neutralizing the ROS in order to maintain the redox levels at higher temperature is well known. These results strongly show the requirement of sufficient levels of GSH for the pigmentations and the preference of the cell in utilizing GSH in redox functioning over detoxification.

3.3.6 Complementation by GRX4 restores the pigmentation of grx4Δ in ade2Δ background

In order to safely conclude how GRX4 play a role in conjugation between GSH and AIR/CAIR, GRX4 complementation experiment was done. This will also confirm its role in red pigmentation.

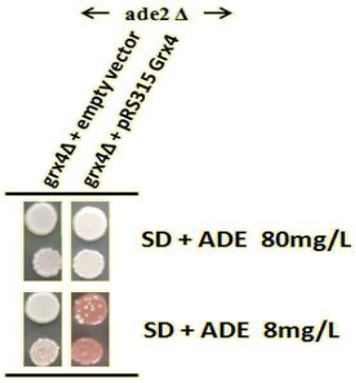

***Fi*gure 3.11**: GRX4 complements the pigmentation defect in *grx4Δade2Δ* mutant

From the figure 3.11, we confirm that GRX4 is the enzyme which plays a role in conjugation of AIR / CAIR with GSH. GRX4 a Glutathione-dependent oxidoreductase, belongs to the monothiol glutaredoxin subfamily. It is involved in radical responsive to hydroperoxide and superoxide and in protecting cells from oxidative damage. GRX4 also appears to play a role in the nucleus as a transcriptional activator. Along with Grx3p, Grx4p binds to Aft1p, the low-iron sensing transc in iron-replete conditions, promoting its dissociation from promoters. The Monothiol glutaredoxin involved in the biogenesis of iron-sulfur clusters (by similarity) binds one iron-sulfur cluster per dimer. This iron-sulfur cluster is bound between subunits, and is complexed by a bound glutathione and a cysteine residue from each subunit. Thus the precise role of GRX4in adenine pigmentation remains unclear. One possibility is a direct involvement in conjugation. However it could also be involved through a still unknown transcriptional regulatory process.

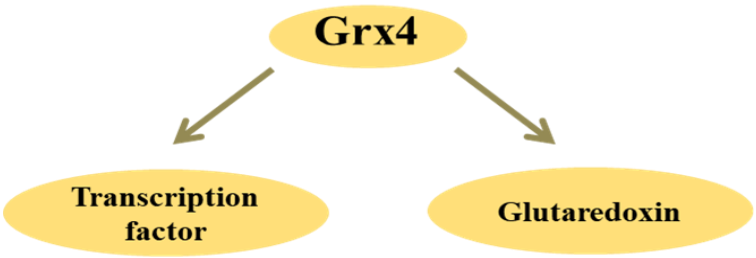

***Fi*gure 3.12**: Major functions of GRX4in cell functioning

3.3.7. A Color table illustrating the pigmentation at different ADE concentrations

	80mg ADE	*8mg ADE*	*8mg ADE + 100µM GSH*	*8mg ADE 30˚C*	*8mg ADE 37˚C*
WT	+ + +	+ + +	+ + +	+ + +	+ + +
ade2Δ	+ + +	+ +	+ +	+ +	+
ade2Δgrx1Δ	+ + +	+ +	+ +	+ +	+
ade2Δgrx2Δ	+ + +	+ +	+ +	+ +	+
ade2Δgrx3Δ	+ + +	+ +	+ +	+ +	+
ade2Δgrx4Δ	+ + +	+ +	+ +	+ +	+
ade2Δgrx5Δ	+ + +	+ +	+ +	+ +	+
ade2Δgrx6Δ	+ + +	+ +	+ +	+ +	+
ade2Δgrx7Δ	+ + +	+ +	+ +	+ +	+
ade2Δtrx1Δ	+ + +	+ +	+ +	+ +	+
ade2Δtrx2Δ	+ + +	+ +	+ +	+ +	+
ade2Δtrx3Δ	+ + +	+ +	+ +	+ +	+
ade2Δgto1Δ	+ + +	+ +	+ +	+ +	+
ade2Δgto2Δ	+ + +	+ +	+ +	+ +	+
ade2Δgto3Δ	+ + +	+ +	+ +	+ +	+
ade2Δprx1Δ	+ + +	+ +	+ +	+ +	+
ade2Δgtt1Δ	+ + +	+ +	+ +	+ +	+
ade2Δgtt2Δ	+ + +	+ +	+ +	+ +	+
ade2Δsrx1Δ	+ + +	+ +	+ +	+ +	+

Better growth (+++), Moderate growth (++), Low growth (+),

Table 3.2: A Color table illustrating the pigmentation at different ADE concentrations.

3.3.8 Investigating the role of post-vacuolar processing of AIR / CAIR-GSH in pigment formation

A second aspect of the ade pigmentation phenotype that has not been adequately investigated or explored is the role of post-vacuolar processing in the pigment formation. We were thus interested to investigate the role of vacuolar enzymes (if any) in the processing of the Glutathione conjugates in the vacuole. An important question was to know if it is the conjugated product in the lower pH and oxidizing environment of vacuole that is giving rise to red pigmentation or if the conjugated product is undergoing some processing inside the vacuole after which it gives red pigmentation. In order to address this, we mined the various peptidases that are localized in the vacuole for those that might be capable of modifying the ADE conjugated product which may result in a red pigmentation. The list of possible peptidases (amino peptidases and carboxipeptidases) which could play a vital role in processing the conjugated product is listed in table 2.

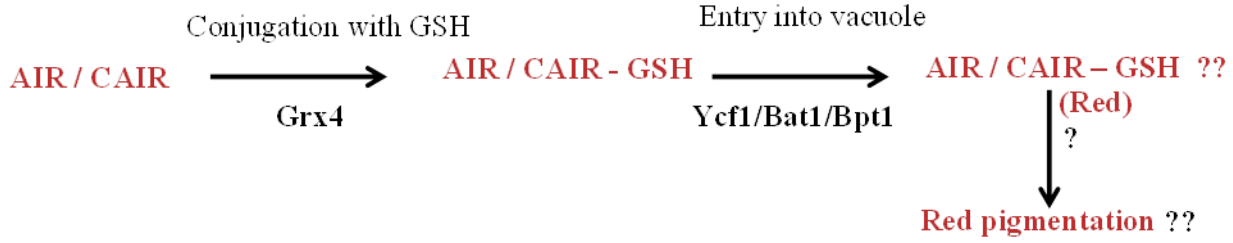

***Fi*gure 3.13**: A schematic illustrating the uninvestigated role of post vacuolar processing.

GENE NAME	DESCRIPTION	FUNCTION
Lap1	Aminopeptidase	Metalloaminopeptidase activity
Lap2	Leucyl aminopeptidase	Aminopeptidase activity
Lap3	Cysteine aminopeptidase	Cysteine-type peptidase activity
Lap4	Vacuolar aminopeptidase	Metalloaminopeptidase activity
Ecm38	Gamma-glutamyltranspeptidase	Glutathione hydrolase activity
Aap1	Arginine / alanine aminopeptidase	Metalloaminopeptidases,
Ybr139	Vacuolar serine-type carboxypeptidase	Serine-type carboxypeptidase activity
Prc1	Vacuolar carboxypeptidase	Serine-type carboxypeptidase activity
Cps1	Vacuolar carboxypeptidase	Carboxypeptidase activity
Pep4	Vacuolar aspartyl protease	Peptidase activity
Kex1	Vacuolar carboxypeptidase	Serine-type carboxypeptidase activity

Table 3.3: A table contains the list of vacuolar peptidases with a function capable of altering the conjugated product. It is to be noted that APE1 is also known as lap4.

3.3.9. Investigating the involvement of the vacuolar peptidases involved in red pigmentation in vacuole

To investigate the role of these different vacuolar peptidases, we procured their knockouts from Euroscarf . Following this deletion of genes *ADE1* and *ADE2* in the different peptidases knockout strains were made to identify if the enzyme involved in the processing the AIR/CAIR conjugate. Although the confirmed presence of pigment would not necessarily eliminate a role for these enzymes in ade pigment formation, an absence of red pigmentation would definitely indicate a role for this enzyme in processing. ADE2::HIS3 disruption cassette was created to disrupt ADE2 gene separately in different peptidases knockout strains.

The growth of yeast colonies were selected on + adenine-HIS plates after transforming them with the required disruption cassette. Finally their phenotype was examined to confirm the disruption (adenine auxotroph), and pigmentation phenotypes on limiting adenine was then examined.

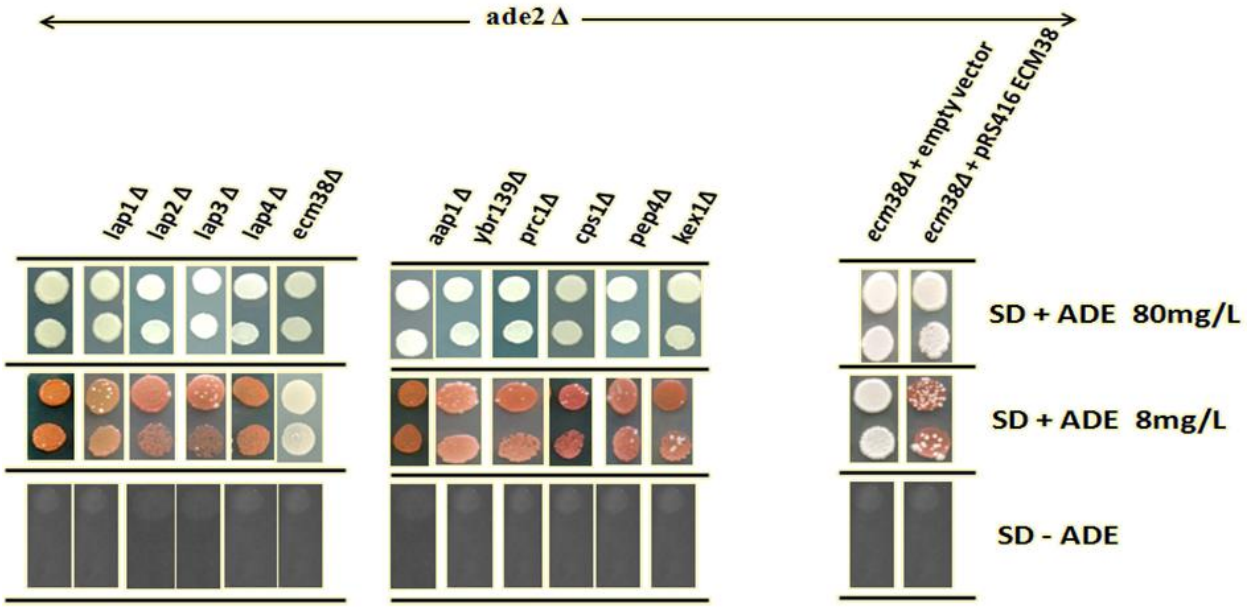

Figure 3.14: Visual screening based study to identify peptidases involved in post-vacuolar processing of the CAIR / AIR – GSH conjugate

We observed that in excess adenine supplementation no red pigmentation is observed. There was no growth observed in the SD-ADE plates as these deletion stains were adenine auxotroph. All the deletions had no defect in pigmentation. However, in the case of *ecm38Δade2Δ* there was no red pigmentation observed even when the adenine concentration was minimal. *ecm38Δ* shows almost complete lack of pigmentation in both *ade1Δ* and *ade2Δ* background.

3.3.10. Involvement of ECM38 in post-vacuolar processing of the CAIR / AIR – GSH conjugate

ECM38 is a ϒ-glutamyl transpeptidase. Being a major glutathione-degrading enzyme, it is involved in detoxification of electrophilic xenobiotics. It also catalyzes the transfer of the ϒ-glutamyl moiety of glutathione (GSH) and other ϒ-glutamyl compounds to amino acids and peptides. It also plays a role in the turnover of the vacuolar GSH, serving as an alternative nitrogen source during nitrogen starvation. Further, an ECM38 complementation experiment was carried out as shown in figure 3.14 to confirm its role in red pigmentation.

3.3.11. Predicted players involved in the red pigmentation in vacuole (*ade* Δ)

It is observed that the amino acids gets recycled while the X (toxic substance) gets accumulated inside the yeast vacuole. The schematic in Figure 3.15 represents the pathway inside the vacuole as we predict it.

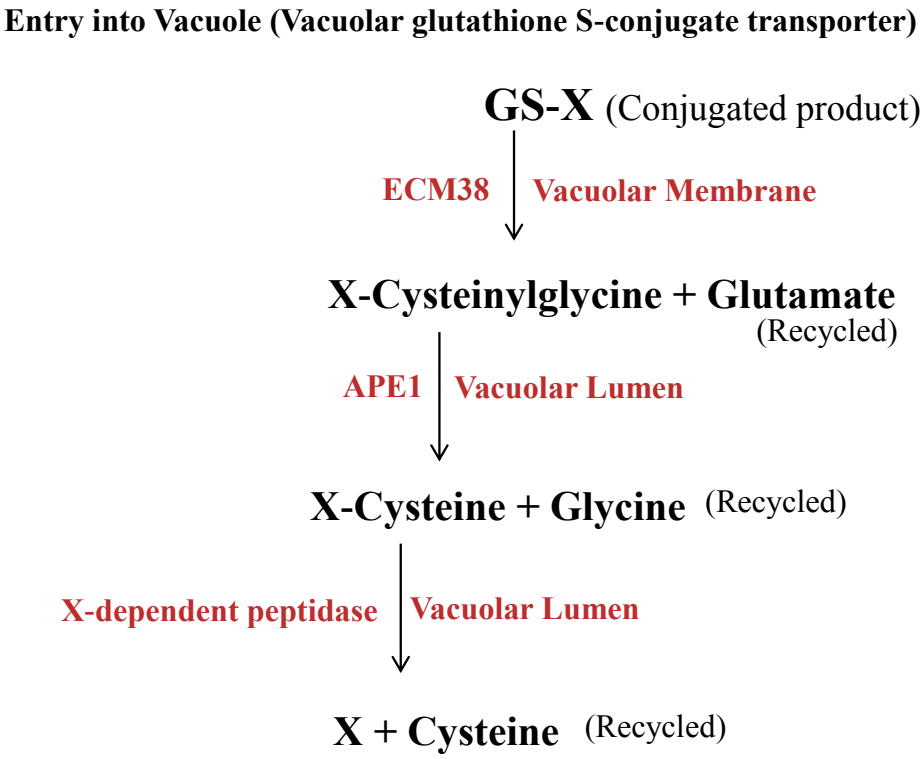

Figure 3.15: A Schematic showing the predicted players involved in the red pigmentation in vacuole (*ade Δ*)

3.4. Conclusion

In this study, we have investigated missing links in the pathway responsible for the red pigmentation present in the *ade1Δ/ ade2Δ* mutants of *Saccharomyces cerevisiae*. One of the missing link is the conjugation step. To identify possible enzymes involved in this step we carried out a deletion analysis of candidate genes that might be involved. We have shown that GRX4 is the likely GST responsible for the AIR/CAIR and GSH conjugation in the cytosol. The second aspect that was investigated was the possible role of vacuolar peptidases in the post-vacuolar processing of the conjugate and the role in pigment formation. Among the various vacuolar peptidases we have shown that, ECM38, a ϒ-glutamyl transpeptidase acts on the AIR/ CAIR - GSH conjugate, thereby catalyzing the transfer of the ϒ-glutamyl moiety present into amino acids and peptides.

Chapter 4: Reconstruction of Felis catus' Felinine biosynthetic Pathway in Saccharomyces cerevisiae.

4.1. Introduction

4.1.1. Felinine – Properties and uses

Felinine is a cysteine thioether found in cat urine. Domestic cats spray urine containing species-specific odor for territorial marking. Felinine (2-amino-7-hydroxy-5,5-dimethyl-4-thiaheptanoic acid), a putative pheromone precursor, is excreted in cat urine. Most mammals have a highly developed olfactory sense. Urinary odorants and pheromones are crucial for chemical communication used in reproduction, territoriality, and conspecific recognition. Felinine also functions as a cat pheromone and is highly valued in odor-based industries. Derivatives of felinine are also found in cat's urine and have odor characteristics. Felinine can also be used as a rat deterrent as rats are biologically programmed to perceive cat pheromone as threat (Papes, Logan and Stowers, *Cell.* 2010).

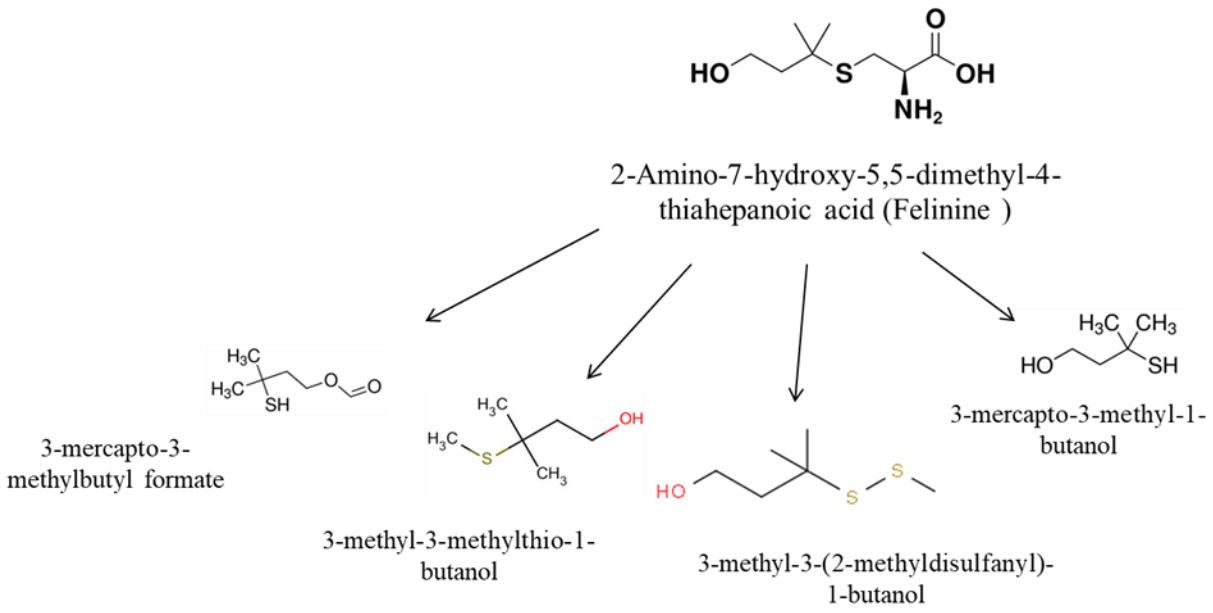

Figure 4.1: Schematic showing various Felinine derivatives

4.1.2. Locations of the putative enzymes involved in felinine biosynthesis in the cat renal system

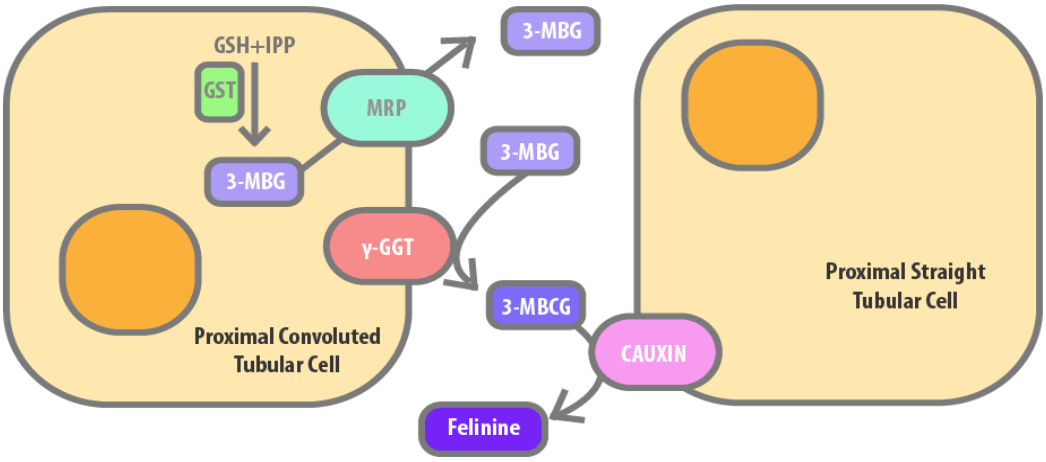

Figure 4.2: A Schematic representation of locations of the putative enzymes involved in felinine biosynthesis in the cat renal system

4.1.3 Felinine biosynthesis in cats

A felinine precursor is present in cat blood as 3-methylbutanol-glutathione (3-MBG) and is formed via a glutathione conjugation reaction between glutathione (GSH) and isopentenyl pyrophosphate (IPP). In general, glutathione S-conjugates such as 3-MBG are converted to cysteinylglycine S-conjugates (3-MBCG) by γ-glutamyl transferase in the kidney (proximal convoluted tubular cells) and the cysteinylglycine S-conjugates are hydrolyzed by cauxin (with proximal straight tubular cells) to give rise to felinine, the precursor of cat pheromone (20).

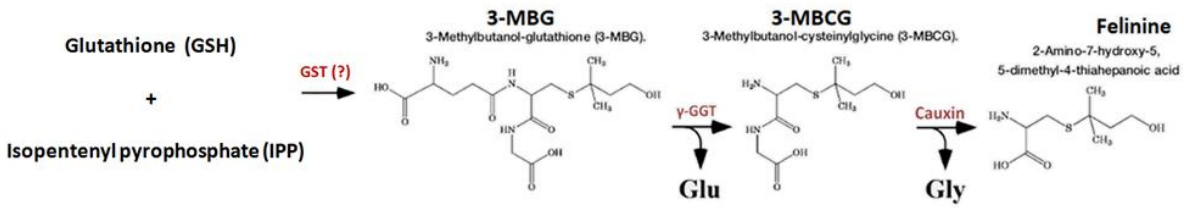

Figure 4.3: An Illustration of the predicted Felinine pathway in cats

4.1.4. Predicting a probable felinine biosynthesis pathway in *S. cerevisiae*

Since GSH and IPP are made in yeast the possibility of reconstructing the felinine pathway in yeast exists. The specific enzyme responsible for the conjugation, GST however needs to be introduced in yeast. As GSTs are a family of enzymes, it is necessary to identify the specific cat GST responsible for the reaction and introduce the gene for this enzyme in yeast. Following the conjugation of GSH to IPP to form the felinine precursor, this precursor needs to be processed to eventually yield felinine. The first enzyme is a followed by a γ-glutamyl transpeptidase followed by a carboxypeptidase. These enzymes are localized in the yeast vacuole.

Therefore the putative GST needed for the conjugation must be introduced in the cytoplasm, which can be further metabolized through the above mentioned pathway after entering the vacuole through the YCF1 pump. These properties of *Saccharomyces cerevisiae* coupled with the fact that their cells use pheromone based intracellular signal transduction pathway for mating made us choose *Saccharomyces cerevisiae* as our model organism for the production of cat pheromone.

4.1.5. Localizations of yeast enzymes which play a role in felinine synthesis

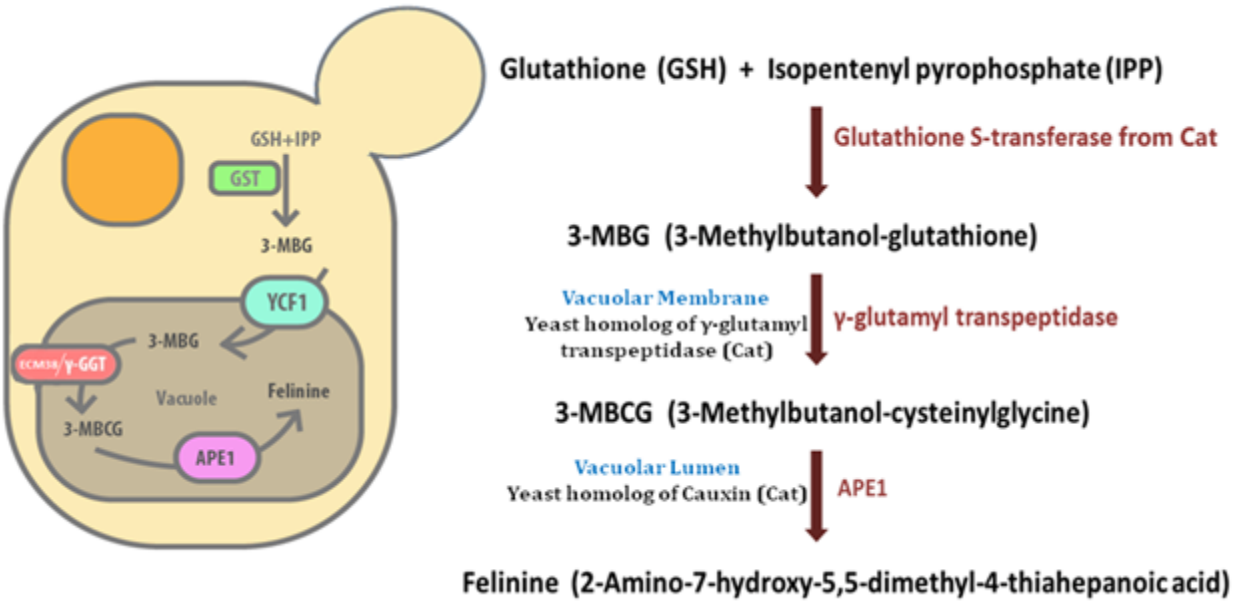

Figure 4.4: A schematic representation of the predicted Felinine pathway in yeast

The figure 4.5 given above shows the proposed schematic pathway for felinine synthesis in *Saccharomyces cerevisiae*.

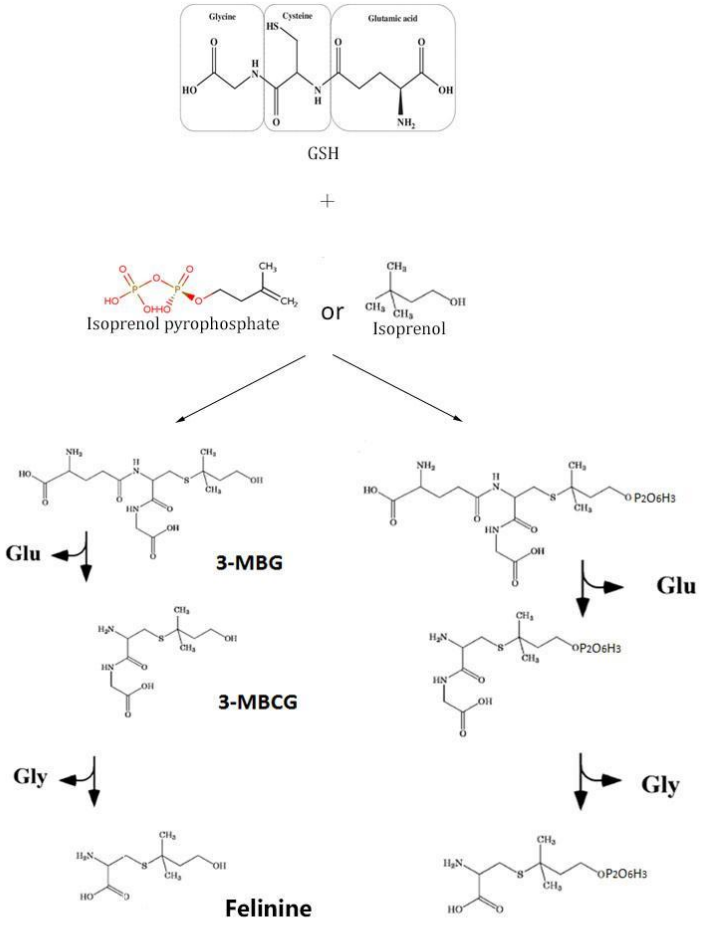

Figure 4.5: Figure illustrating the possible pathways for felinine production in yeast

4.2. Objective

The overall goal of this project was to reconstruct the *Felis catus'* Felinine biosynthetic Pathway in *Saccharomyces cerevisiae*.

Towards this goal the following specific objectives were identified.

Strategy and approach for reconstructing the Felinine pathway in *Saccharomyces cerevisiae* :

1. Identification of putative GST involved in felinine pathway that conjugates IPP with glutathione.
2. Cloning and expression of *Felis catus'* GST gene in *Saccharomyces cerevisiae.*
3. Evaluation of putative GST *in vitro* desired enzyme activity.
4. Evaluation of felinine production in yeast extracts
5. Roles of endogenous yeast enzymes in felinine production.
6. Animal Testing

4.3. Results and Discussions

4.3.1. Identification of putative Glutathione-S-Transferase (GST) involved in felinine pathway that conjugates IPP with GSH

Glutathione-S-transferases is a large superfamily of proteins that contains several subclasses. To examine if contained a unique GST we carried out sequence comparison using BLAST with all human GSTs against cat genome. These enabled us to list out all the cat GSTs but no unique GST was identified.

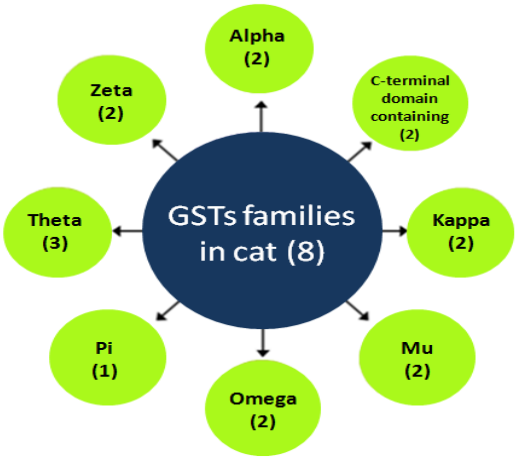

Figure 4.6: Figure illustrating the GSTs families in *Felis catus*

Homo sapiens (taxid:9606)		*Felis silvestris catus* (taxid:9685)			*Saccharomyces cerevisiae* (taxid:4932)		
Protein	**Class**	**Protein**	**Class**	**E-Value**	**Protein**	**Class**	**E-Value**
GST	A1	GST	A4	6.00E-88	No significant similarity found	-	-
GST	CD	GST	CD	0	No significant similarity found	-	-
GST	K1	GST	K1	1.00E-144	FIR1p [*Saccharomyces cerevisiae* YJM1332]	-	1.8
GST	M3	GST	M3	7.00E-154	Uncharacterized YPR136C	-	0.64
		GST	M4	3.00E-85	No other match found	-	-
GST	O1	GST	O1	4.00E-157	No significant similarity found	-	-
GST	P1	GST	P	5.00E-139	No significant similarity found	-	-
GST	T1	T isoforms ignored	-	-	URE2p	-	0.002
GST	T2B	elongation factor 1-gamma	-	3.00E-03	Protein URE2	-	0.23
GST	Z1	hematopoietic prostaglandin D synthase	-	3.30E-02	No significant similarity found	-	-
MGST	1	prostaglandin E synthase		1.00E-29	No significant similarity found	-	-

Table 4.1: Table illustrating the BLAST results for Human GSTs and cat GSTs

Cat		*Homo sapiens* (taxid:9606)			*Saccharomyces cerevisiae* (taxid:4932)		
Protein	**Class**	**Protein**	**Class**	**E-Value**	**Protein**	**Class**	**E-Value**
GST	A4	GST	A4	4.00E-153	No significant similarity found	-	-
GST	CD	GST	CD	0	No significant similarity found	-	-
GST	K1	GST	K1-1	2.00E-143	No significant similarity found	-	-
GST	M3	GST	M3 (brain)	2.00E-153	Uncharacterized YPR136C	-	0.26
GST	O1	hCG1646871	-	4.00E-129	No significant similarity found	-	-
GST	P1	GST	P	2.00E-124	No significant similarity found	-	-
GST	T4	hCG41097	-	3.00E-137	No significant similarity found	-	-
GST	Z1	GST	Z1	7.00E-147	No significant similarity found	-	-
MGST	T2	Leukotriene C4 synthase	-	6.00E-30	No significant similarity found	-	-

Table 4.2: Table illustrating the BLAST results for cat GSTs and human GSTs

From the BLAST analyses, we found out that no GST was found to be specific to cat GSTs in comparison to the well studied human GSTs.

4.3.2GSTM3 picked as a putative GST involved in felinine biosynthesis based on tissue metabolites localizations

Tissue-level expression profiles of the GSTs in comparison with the tissue content of the involved metabolites revealed that the kidney and bladder was the major locations where felinine synthesis was occurring.

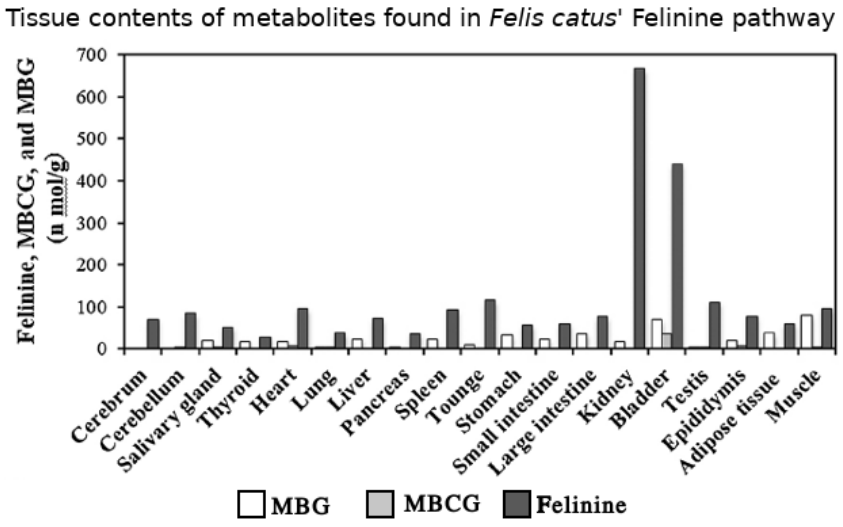

Figure 4.7: Figure reproduced from A. Futsuta et. al., *2018* illustrating the Tissue contents of metabolites in cats

We next determined which GSTs were reported to be localized to the kidney and bladder. Based on the above criteria, GSTM3 turned out to be the best candidate among all the cat GSTs. Therefore, GSTM3 was taken as the putative GST to test the GSH-IPP conjugation and all further experiments were carried out using GSTM3.(Biochemical and Biophysical Research Communications 463 (2015) 650-655)

4.3.3 Experimental approach for reconstructing the felinine pathway in yeast

4.3.3.1. Codon optimization, custom synthesis and cloning of GSTM3 gene from *Felis catus* into the yeast expression vector

GSTM3 gene from *Felis catus* was custom synthesized and codon optimized for expression in *Saccharomyces cerevisiae* (IDT technologies). The size of GSTM3 was 780 nucleotides. For expression in yeast the custom synthesised gene was amplified along with an HA-tag with restriction sites. The gene was cloned downstream of the TEF promoter with a downstream CYC terminator.

The insert band obtained via gel purification after PCR amplification was subjected to digestion with the restriction enzymes EcoRI and XbaI. Similarly, the plasmid backbone pRS313-TEF was also digested with the same restriction enzymes. Finally the digested products were ligated at 16°C for 16 hours (hrs) and were used for transformation in *E.coli*. Plasmids were isolated, and the screening of positive clones was achieved through restriction digestion. The gene GSTM3 was successfully cloned in yeast expression vector (pRS313-TEF) and the clone was sequence verified.

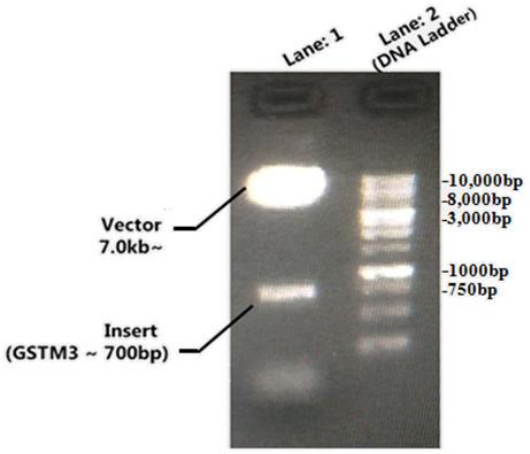

Figure 4.8: Cloning of GSTM3 in yeast expression vector (pRS313-TEF).

4.3.3.2. **Validation for GSTM3 expression in *Saccharomyces cerevisiae***

Plasmids containing GSTM3 were transformed in *Saccharomyces cerevisiae* under the TEF promoter. In order to check the protein expression, we performed western blot using anti-HA mouse antibody. The size of the protein was found to be 25 kDa which corresponds to the expected cat GSTM3 protein.

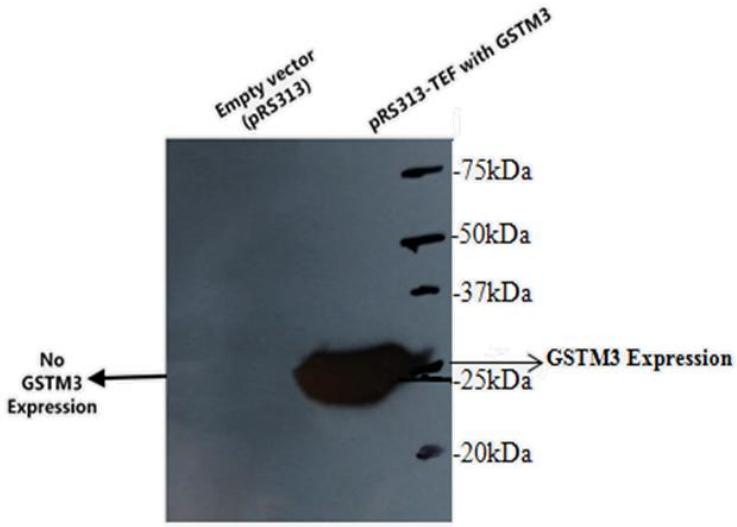

Figure 4.9: Western Blot for checking the expression of cat GSTM3 in yeast

In order to check the protein expression, we performed western blot of the constitutively expressed protein GSTM3 tagged with HA tag and FLAG tag on its N- terminal and C- terminal respectively. The plasmid (pRS313-TEF) with GSTM3 and the empty plasmid (pRS313-TEF) was transformed in wild type yeast, and the 1.0 OD_{600}cells were harvested and western blotting was done by using anti-HA mouse antibody to probe the HA tag. A specific band at 25 kDa was observed which corresponds to GSTM3 protein. This confirms that the cat GSTM3 was expressed in *Saccharomyces cerevisiae*.

4.3.3.3. ***Protein purification and In vitro analysis of the GST conjugation***

In order to purify the GSTM3 and i*n-vitro* evaluation for the conjugation between GSH which IPP through GSTM3. GSTM3 gene was cloned into the *E. coli* protein expression vector (pET28a+) using the restriction enzymes, this enabled the protein to be HIS-tagged. The figure given below shows the agarose gel picture of the double digested recombinant vector. In the figure, Lane 1 represents the run of the digested recombinant plasmid and lane 3 represents the marker (1kb DNA Ladder). From lane 1, we can see the band-size of the insert fragment at around 780 bp and the digested plasmid backbone at around 5.0 kb. Thereby the double digestion using EcoRI and NdeI validated the successful cloning of the insert GSTM3 in pET28a(+). Further the clones were successfully sequence verified.

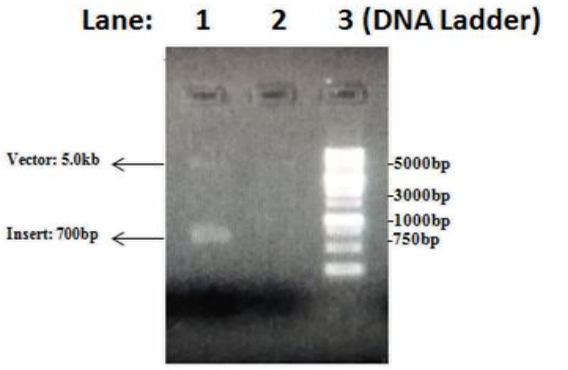

Figure 4.10: Cloning of GSTM3 in protein expression vector pET28a(+).

4.3.3.4. **Protein purification and *In vitro* analysis of the GST conjugation.**

The cloned pet28(+) was transformed into BL21 strain of *E.coli* for purification. The figure below shows the coomassie plot of the concentrated GSTM3 (25kDa) using Ni-NTA column. The purified protein was used to evaluate the enzymatic property of the protein.

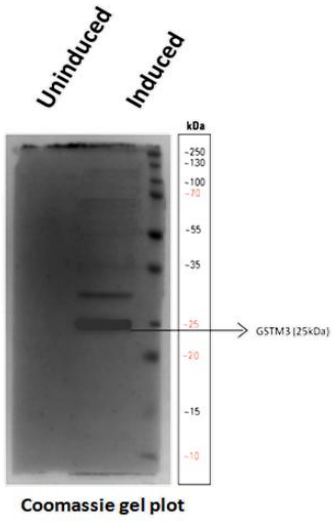

Figure 4.11: The coomassie gel plot showing the concentrated band of GSTM3 at around 25kDa.

4.3.3.5. *In vitro* enzymatic assay to check GSTM3 activity with GSH and IPP

An enzymatic assay was performed with the purified GSTM3 along with the commercially obtained substrates (GSH, IPP, Isoprenol (Iso)). The specificity of the purified GSTM3 towards isoprenl, IPP, and the standard GST substrate CDNB (1-Chloro-2,4-dinitrobenzene) was examined and a comparative analysis was also carried out with a commercial obtained GST, equine GST(CAS number: 50812-37-8; EC number 2.5.1.18). CDNB conjugation to GSH was detected by absorbance at 340nm. To detect 3-MBG formation, we first ran a wavelength scan of this product formed to determine the absorption maxima. This is shown below. The Absorption maxima were obtained at 570nm and this wavelength was used for the following reaction.

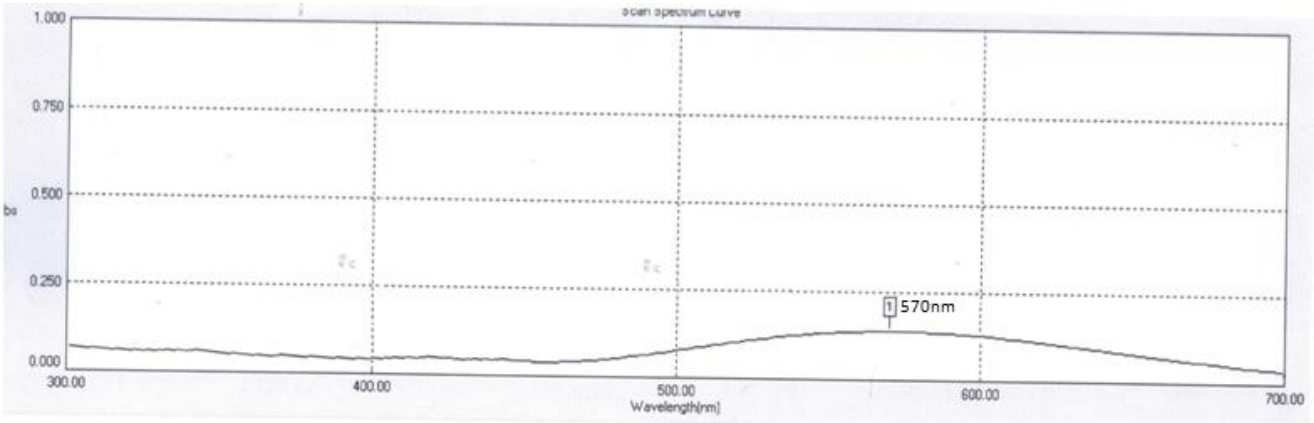

Figure 4.12: Normalized absorption spectra for varying concentrations of 3-MBG

Specific activity data of reactions in units/mg protein	
Control	0
IPP+stGST	11.93
IPP+GSTM3	18.71
Iso+stGST	14.41
Iso+GSTM3	13.26
CDNB+stGST	24.21
CDNB+GSTM3	12.46

Table 4.3: Table illustrating the Specific activity data of reactions in units/mg protein

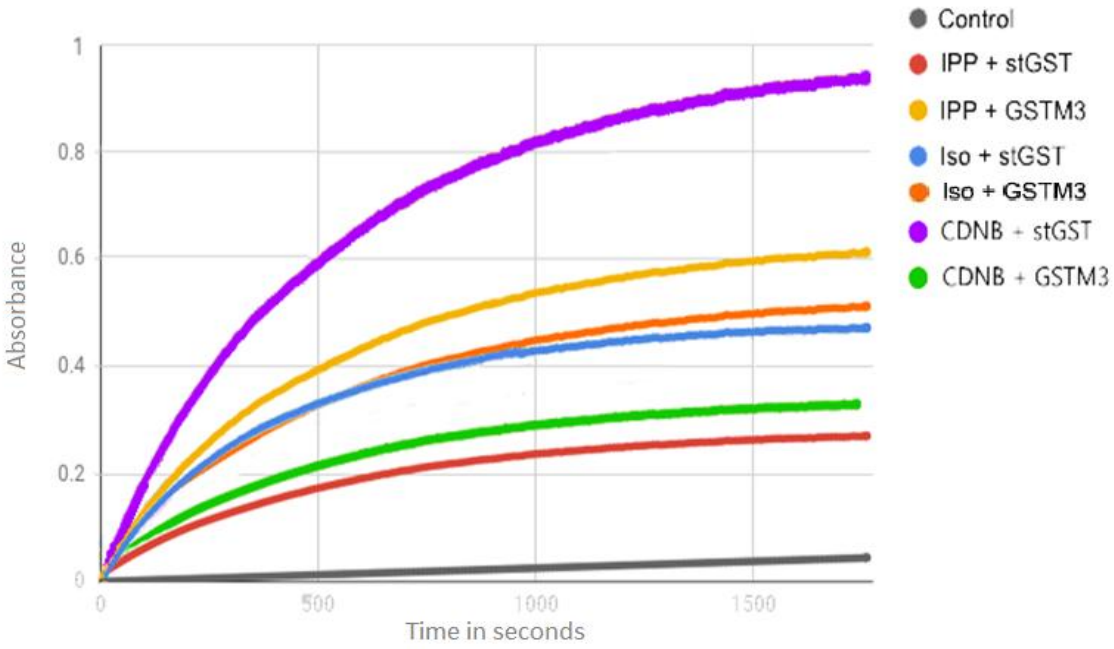

Figure 4.13: Plot obtained from the enzymatic assay to check enzyme activity.

4.3.3.6 Analysis of the enzymatic assay plot :

In the reaction of IPP with stGST and GSTM3, We observe that the absorbance levels of GSTM3 is higher than that of stGST. This is due to the fact that GSTM3 is designed to act upon IPP and therefore is the most active.

In the case of Isoprenol, we see that although the reaction rates are better than that of IPP and stGST, they are less reactive than the IPP-GSTM3 reaction. The absorbance levels of Isoprenol reactions with stGST and GSTM3 are almost equal therefore no conclusive inference can be made regarding the specificity on Isoprenol. In the case of CDNB reaction with stGST and GSTM3, we see that the reaction with stGST forms the most product compared to all of the others they both are positive controls. The CDNB reaction with GSTM3 however has lesser reactivity compared to stGST and the IPP GSTM3 reaction.

4.3.3.7. Validation of Felinine expression in Yeast: HPLC Analysis

To evaluate felinine production in yeast, HPLC analysis of the cell lysate was performed in order to verify the production of Felinine using appropriate solvent systems.

The solvent system was chosen to be acetonitrile:trifluoroacetic acid: water (10:0.1:89.9 v/v). The cell culture was grown for 3 days at 30 °C as the culture reached saturation nearly on the third day. Cell lysis was performed on the third day and sample preparation was done as per the protocol stated below. Peaks obtained from the cell lysate were analyzed for the production of felinine.

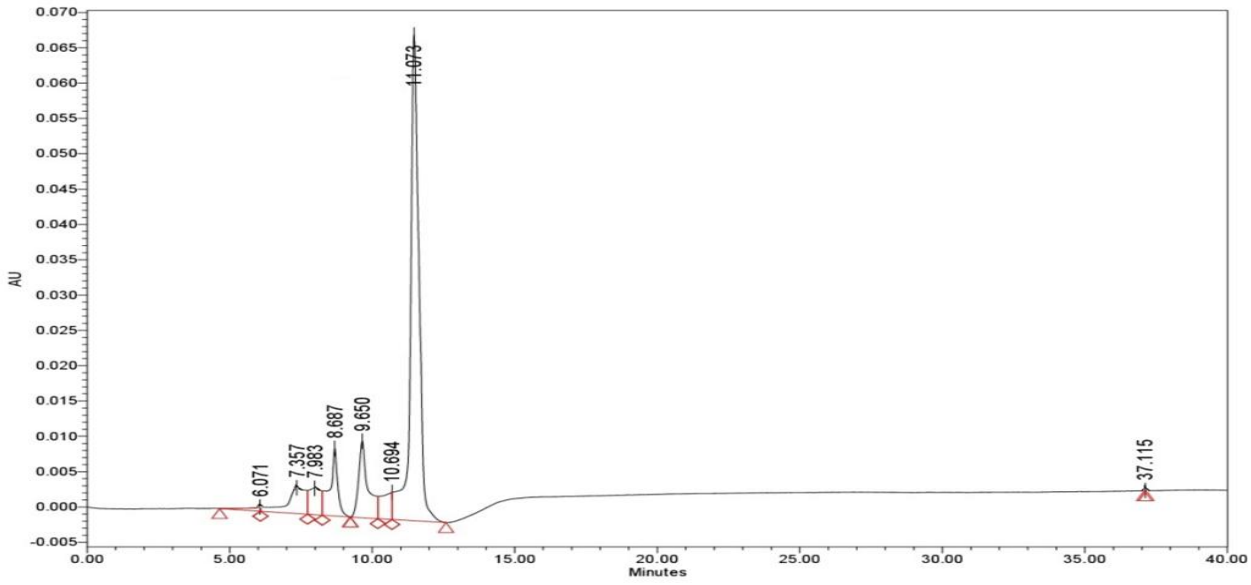

Figure 4.14: Standard containing Felinine

Here, we observe that there is a large peak at 11.073 this peak is characteristic of felinine. Therefore, we use this peak for further comparisons.

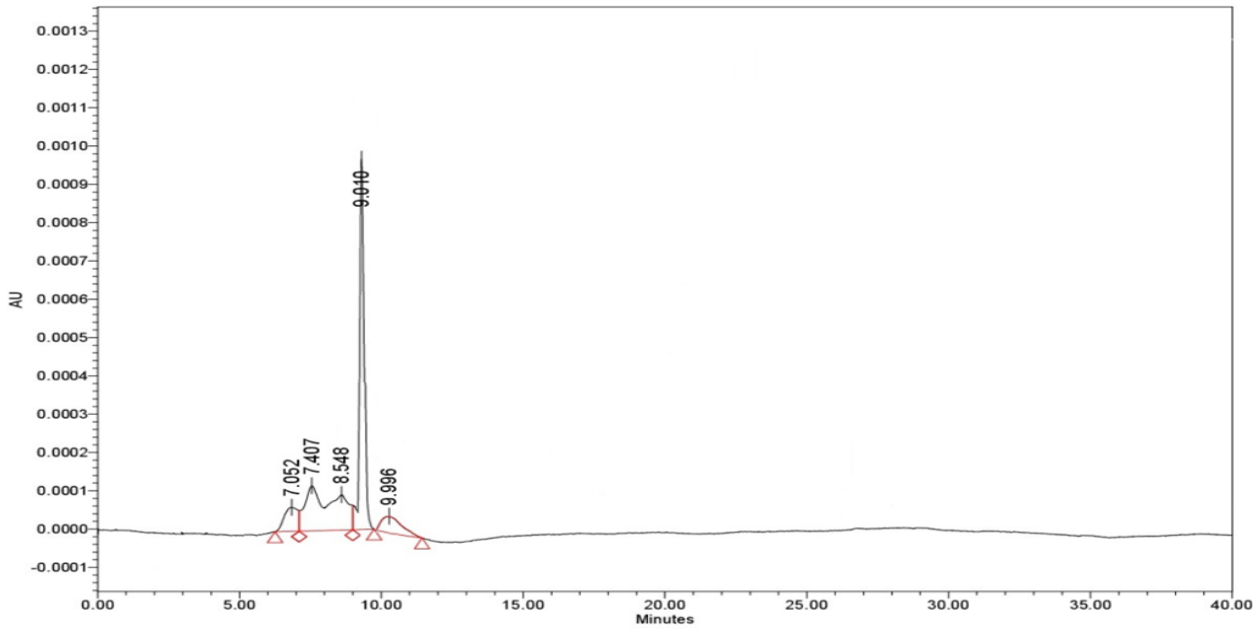

Figure 4.15(a): Wild type yeast having no GSTM3 expression

Here in the HPLC plot figure shown above, we observe that there no peak at 11. 073. This absence of Felinine peak implies the absence of Felinine in the wild type yeast.

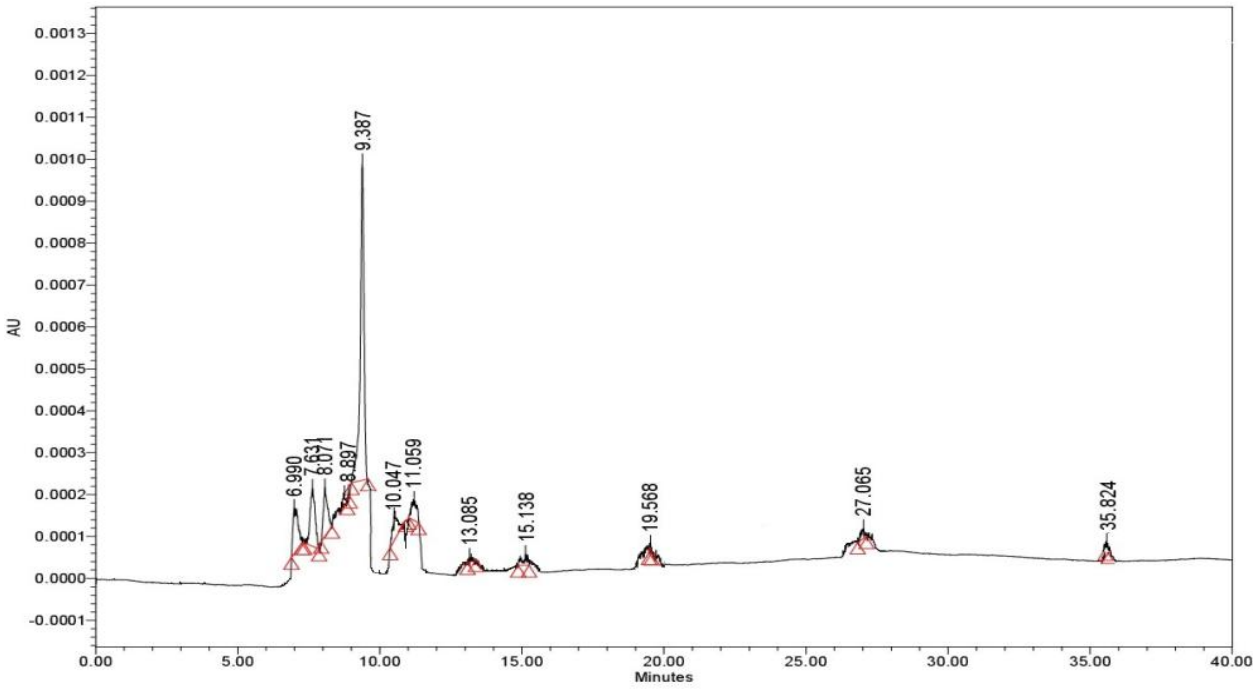

Figure 4.15(b): Recombinant yeast with GSTM3 expression

In the HPLC plot figure given above of the recombinant yeast, we see that there is a peak at 11.059. This peak is similar to the felinine peak but is slightly shifted due to experimental errors. In order to confirm the presence of Felinine, a spiking experiment was done and its results were noted.

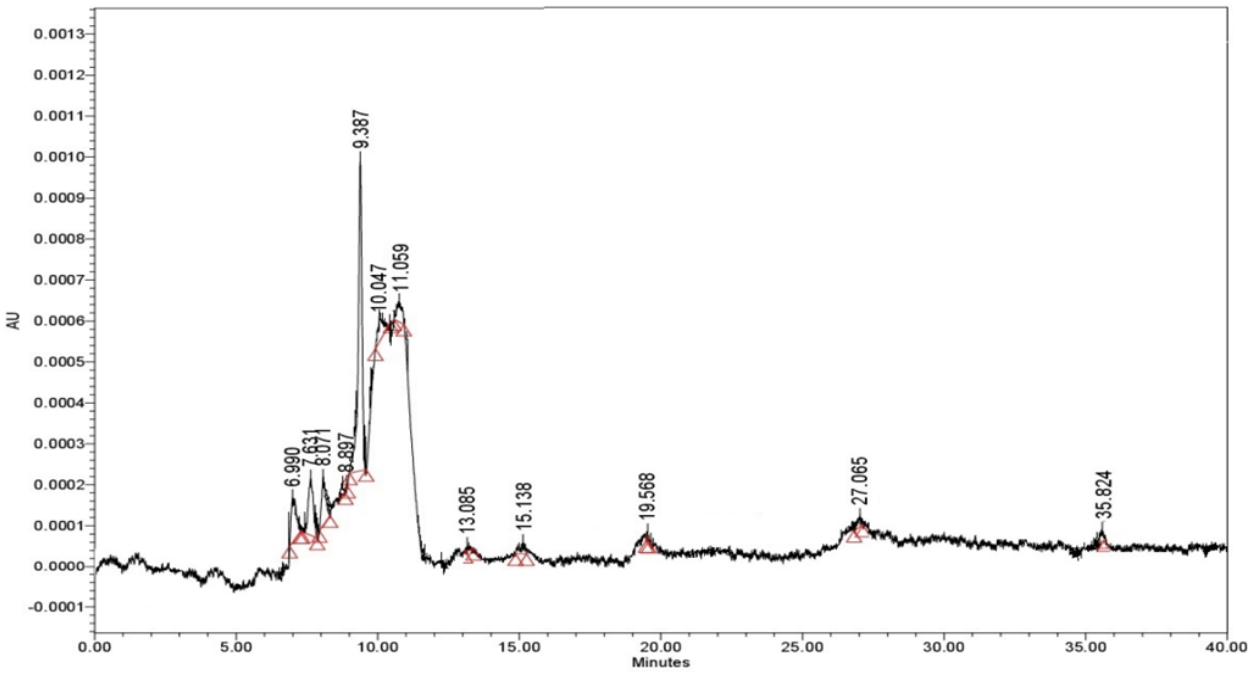

***Figure 4.16*:** Recombinant yeast with GSTM3 expression spiked with felinine standard

In this HPLC plot, we see that the 11.059 peak observed in the recombinant yeast has risen upon addition of Felinine standard to the sample. This confirms the presence of Felinine in the recombinant yeast.

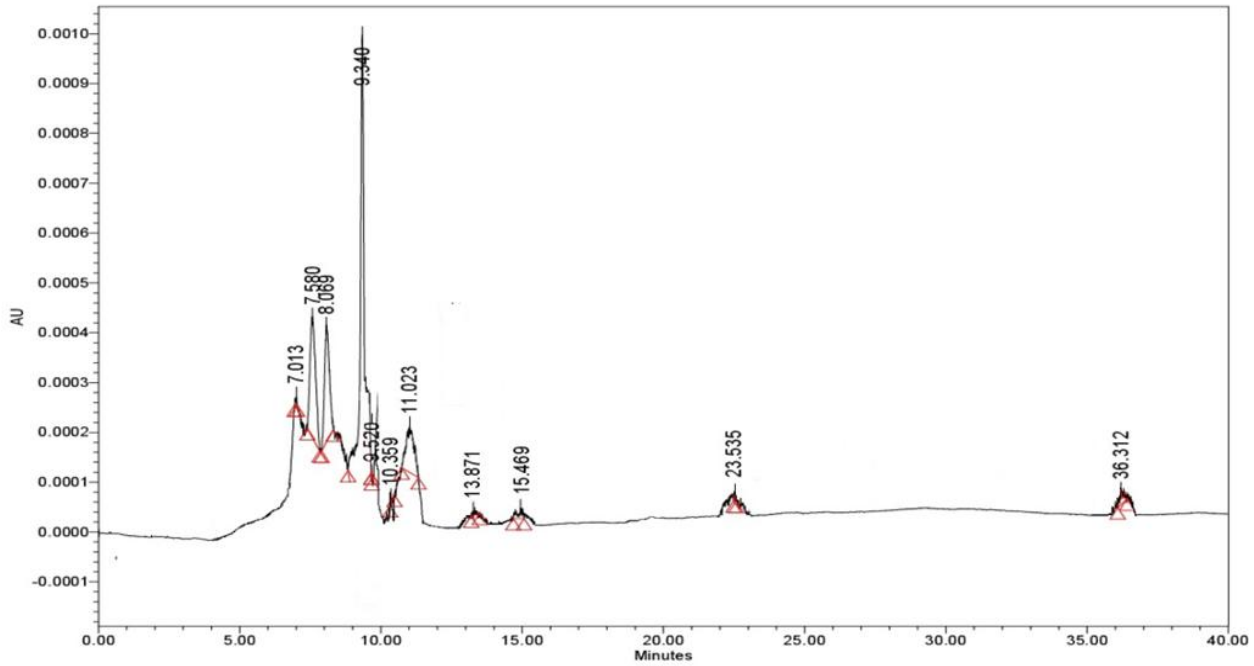

***Figure 4.17*:** Wild type yeast having tHMG1 expression and GSTM3 expression

In order to increase the production of Felinine, we increased IPP flux by truncated HMG over expression. In this HPLC plot, we see that the 11.023 peak observed in the recombinant yeast has risen. This confirms the presence of increase in Felinine production upon increasing the IPP flux in the recombinant yeast.

4.3.3.8. Evaluation of felinine production in *Saccharomyces cerevisiae* using HR-MS

Molecular mass of felinine is 207.2955. In order to further validate the presence of Felinine, Mass spectrometry from sample at 11.0 retention time was performed with in DMSO and Acetonitrile as the solvent.

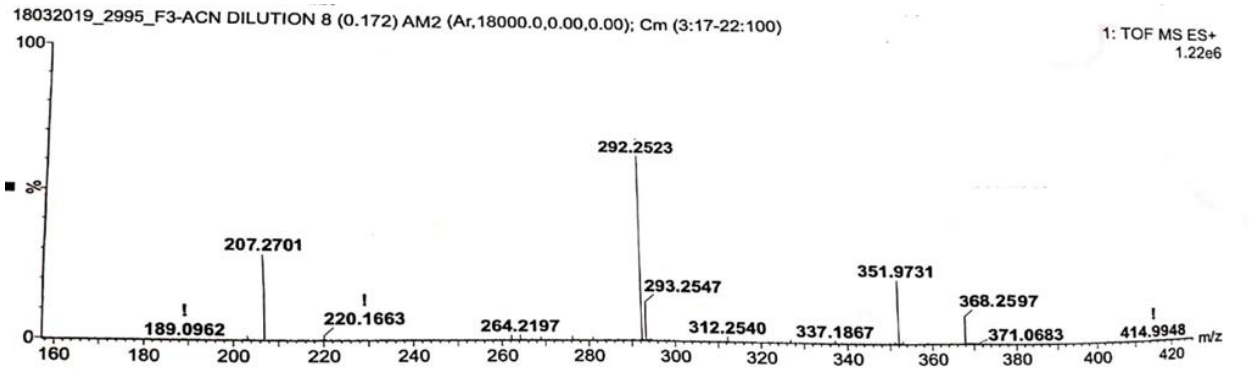

***Figure 4.18*:** Mass spectrometry of recombinant yeast with GSTM3 expression in Acetonitrile solvent

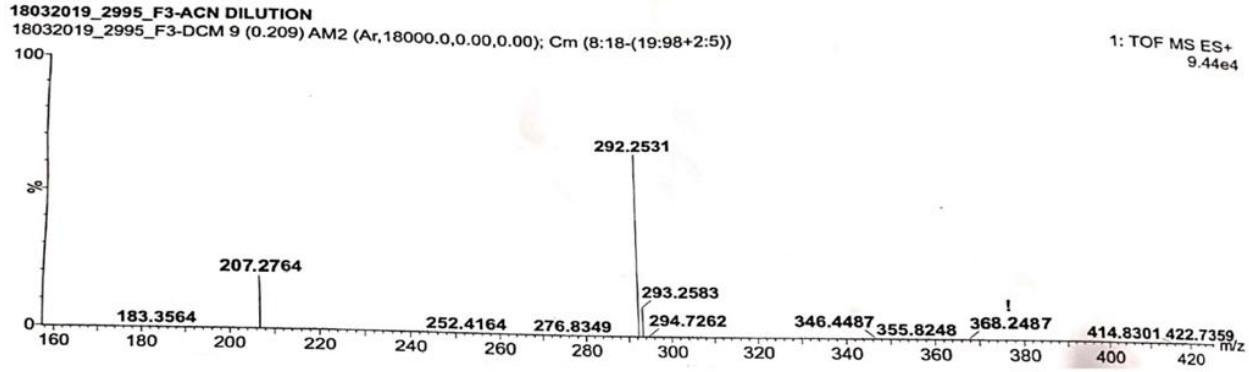

***Figure 4.19*:** Mass spectrometry of recombinant yeast with GSTM3 expression in DMSO solvent

Here we observe that there is a peak corresponding to a molar mass of 207.27 this molar mass corresponds to that of felinine and hence production of felinine in the recombinant yeast is verified.

4.3.3.9. Evaluation of felinine production in different deletion background using HPLC

In order to validate the predicted pathway for the production of felinine, several deletions were carried out independently along the pathway and the effect of this deletion on the production of Felinine was noted. The effects observed were compared to the predicted effects in order to validate the pathway proposed.

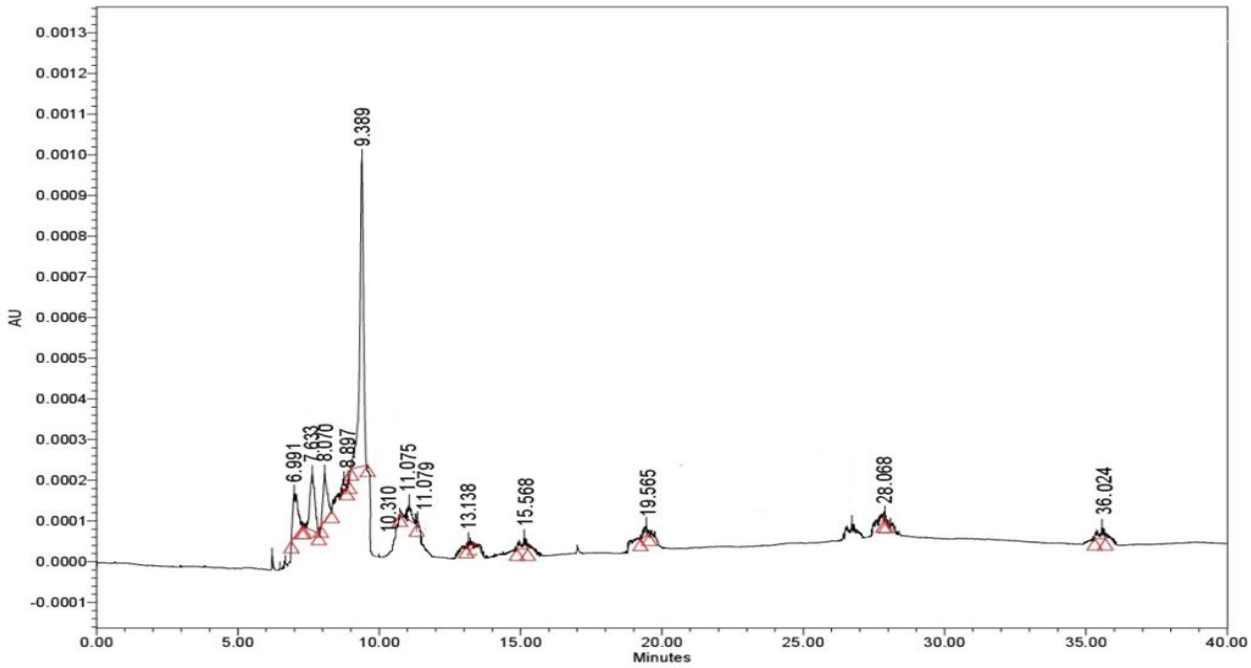

Figure 4.20: HPLC of *ycf1Δ* strain with GSTM3 expression

In this HPLC plot, we see that there is a peak at 11.079 corresponding to the presence of felinine in the recombinant yeast. However compared to the undeleted recombinant strain, the *ycf1Δ* strain has lower levels of Felinine. This is due to the fact that although *ycf1* transporter is not present, there are several other GSH conjugate pumps which are capable of transporting the GSH-IPP conjugate.

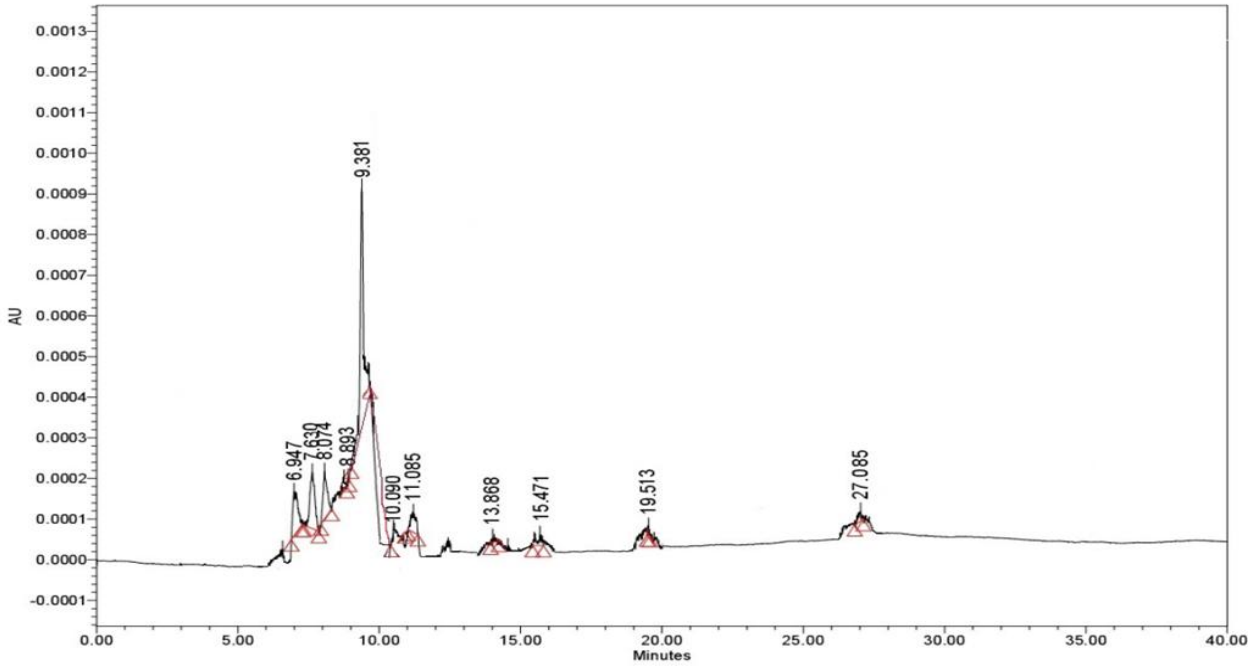

Figure 4.21: HPLC of the *ecm38Δ* strain with GSTM3 expression

In this HPLC plot, we see that there is no peak at 35 but all other HPLC plots appear to have it. This peak may correspond to the presence of 3mbcg which we predict will not be formed in the *ecm38Δ* strain. However no definite information can be extracted without performing mass spectrometric analyses. In addition to these, we can also see that there is peak around 11.097 corresponding to the presence of Felinine. This peak can be attributed to the presence of redundant genes which may perform the activity corresponding to ECM38.

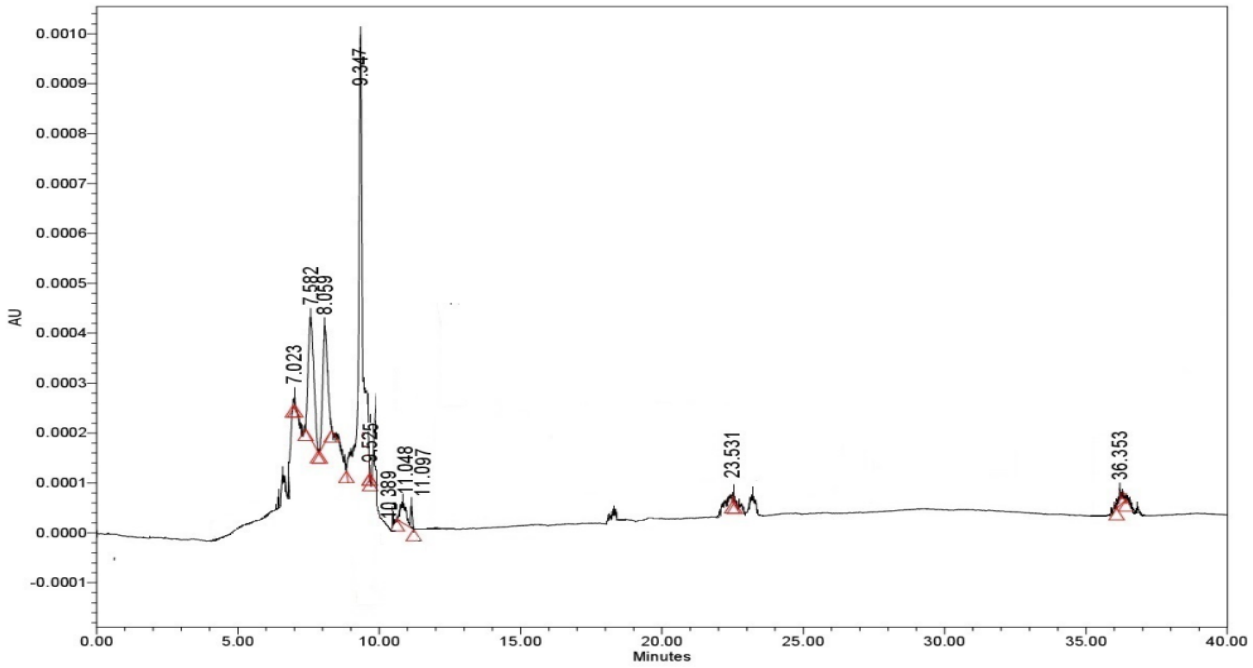

Figure 4.22: HPLC of *ape1Δ* strain with GSTM3 expression Felinine pek dropped many other peaks missing.

In this HPLC plot, we see that the Felinine peak at 1.097 has dropped significantly. Further, there are many peaks missing which all the other HPLC plots appear to have. These peaks may correspond to the various felinine derivatives which require *APE1Δ* for their synthesis. However no definite information can be extracted without performing mass spectrometric analysis.

4.4. Conclusion:

In conclusion, we have successfully reconstructed the cat felinine biosynthetic pathway in yeast. Further we have identified the cat GST responsible for the GSH-IPP conjugation in the nephron to be GSTM3. Further, we have validated the functioning of GSTM3 and have checked for the production of Felinine. The homologs of Gamma GGT, Cauxin in yeast namely ECM38 and APE1 respectively worked as expected to yield Felinine.

Chapter 5: References

1. Penninckx MJ. An overview on glutathione in Saccharomyces versus non-conventional yeasts. FEMS Yeast Research. 2002.
2. Demirkol O, Ercal N. Glutathione. In: Handbook of Analysis of Active Compounds in Functional Foods. 2012.
3. Ketterer B, Coles B, Meyer DJ. The role of glutathione in detoxication. Environ Health Perspect. 1983;
4. Douch PGC, Buchanan LL. Glutathione conjugation of some xenobiotics by ascaris suum and moniezia expansa. Xenobiotica. 1978;
5. Rebbeor JF, Connolly GC, Dumont ME, Ballatori N. ATP-dependent transport of reduced glutathione on YCF1, the yeast orthologue of mammalian multidrug resistance associated proteins. J Biol Chem. 1998;
6. Bachhawat AK, Thakur A, Kaur J, Zulkifli M. Glutathione transporters. Biochimica et Biophysica Acta - General Subjects. 2013.
7. Bachhawat AK, Kaur A. Glutathione Degradation. Antioxid Redox Signal. 2017;
8. Kaur H, Ganguli D, Bachhawat AK. Glutathione degradation by the alternative pathway (DUG pathway) in *Saccharomyces cerevisiae* is initiated by (Dug2p-Dug3p)2 complex, a novel glutamine amidotransferase (GATase) enzyme acting on glutathione. J Biol Chem. 2012;
9. Meister A. Glutathione, ascorbate, and cellular protection. Cancer Res. 1994;
10. Sharma KG, Kaur R, Bachhawat AK. The glutathione-mediated detoxification pathway in yeast: An analysis using the red pigment that accumulates in certain adenine biosynthetic mutants of yeasts reveals the involvement of novel genes. Arch Microbiol. 2003;
11. Strange RC, Spiteri MA, Ramachandran S, Fryer AA. Glutathione-S-transferase family of enzymes. Mutat Res - Fundam Mol Mech Mutagen. 2001;
12. Dasari S. Glutathione S-transferases Detoxify Endogenous and Exogenous Toxic Agents-Minireview. J Dairy, Vet Anim Res. 2017;
13. Kostaropoulos I, Papadopoulos AI, Metaxakis A, Boukouvala E, Papadopoulou-Mourkidou E. Glutathione S-transferase in the defense against pyrethroids in insects. Insect Biochem Mol Biol. 2001;
14. Gertsch J. Glutathione-s-transferase. In: xPharm: The Comprehensive Pharmacology Reference. 2011.
15. Lu SC. Regulation of glutathione synthesis. Molecular Aspects of Medicine. 2009.

16. Baudouin-Cornu P, Lagniel G, Kumar C, Huang ME, Labarre J. Glutathione degradation is a key determinant of glutathione homeostasis. J Biol Chem. 2012;

17. Papes F, Logan DW, Stowers L. The Vomeronasal Organ Mediates Interspecies Defensive Behaviors through Detection of Protein Pheromone Homologs. Cell. 2010; 18.

18. Kaur AW, Ackels T, Kuo TH, Cichy A, Dey S, Hays C, et al. Murine pheromone proteins constitute a context-dependent combinatorial code governing multiple social behaviors. Cell. 2014;

19. Rutherfurd KJ, Rutherfurd SM, Moughan PJ, Hendriks WH. Isolation and characterization of a Felinine-containing peptide from the blood of the domestic cat (*Felis catus*). J Biol Chem. 2002;

20. Miyazaki M, Yamashita T, Suzuki Y, Saito Y, Soeta S, Taira H, et al. A Major Urinary Protein of the Domestic Cat Regulates the Production of Felinine, a Putative Pheromone Precursor. Chem Biol. 2006;